Experiments and Modeling of Pulp Mat Formation

By
Jinsong Wang, B. Eng., M. Eng.

A Thesis
Submitted to the School of Graduate Studies
in Partial Fulfillment of the Requirements
for the Degree Doctor of Philosophy

McMaster University

This thesis is dedicated to my wife Liwen, to my parents and my brother

Doctor of Philosophy (2001)

McMaster University
Hamilton, ONT, Canada

TITLE: Experiments and Modeling of Pulp Mat Formation

AUTHOR: Jinsong Wang, B. Eng (Tsinghua University, CHINA)
M. Eng. (North Carolina A&T State University, USA)

SUPERVISOR: Professors Andrew Hrymak and Robert Pelton

NUMBER OF PAGES: xii,97

ABSTRACT

In this dissertation, new insights into dispersed air, surfactant and defoamer effects on pulp mat formation in brownstock washing are described based on extensive experimental research. Observations of bubble behavior and channel formation are used to explain the relationship between the presence of dispersed air and the resulting low water drainage rates from the pulp pad. The work provides new understanding of the mechanism of dispersed air effect on pulp washing.

A new pulp mat water permeability model is also included in this dissertation. The model covers a wider pulp fiber concentration range than previous models in the literature.

A systematic experimental investigation of pulp mat formation from dilute suspensions provides concentration profiles and mat thickness as a function of time. Dynamic fiber concentration profiles along the mat formation direction were inferred from standard images using a grayscale analysis calibrated against a set of known concentrations. A modified semi-empirical filtration model, based on the work of Tiller et al, was applied to compressible porous pulp fiber mat formation, and fits the experimental results very well. With this newly developed model, it is easy to calculate the capacity of a pulp washer at varied operating conditions. This model can be used for process optimization and control and make it possible to further improve the pulp washer efficiency.

PREFACE

The majority of the work involved in completing this thesis is summarized in Chapters 2 to 5. The format of this thesis was chosen with the intention that each of these chapters will be submitted, as is, for publication in the literature. To aid the reader in keeping a sense of continuity with this work, an introductory chapter and a generalized summary have also been added. The appropriate references to the journals are given at the end of each of these chapters. The content of these published chapters has been kept intact, but slight modifications in the text and figures have been made in order to provide consistency throughout the thesis.

ACKNOWLEDGMENTS

I would like to express my deepest gratitude to Dr. Andrew Hrymak and Dr. Robert Pelton, my two supervisors. Without their patient guidance and continual encouragement this dissertation would exist only in my dreams.

Next, I would like to acknowledge funding from the Natural Sciences and Engineering Research Council and support and collaboration from Dorset Industrial Chemicals.

Next, I would like to thank Yongmoon Kwon, Jeff Hubert, and Joe Maiolo. They were my partners and buddies in this research group for each period of time. A lot of research results resulted from their hard work.

Lastly, I would like to thank, Shiping Liu, Dr. Yale Sheng for useful discussions of flow mechanics, and also the advice from Prof. Stolle through my committee meetings.

TABLE OF CONTENTS

LIST OF FIGURES

LIST OF FIGURES (Continued)

LIST OF FIGURES (Continued)

LIST OF TABLES

NOMENCLATURE

k	empirical constant for equation 3-2
m	constant in equation 5-11
n	constant in equation 5-11
q	local water flux (m^3/m^2)
q_s	downward flux of pulp fiber (m^3/m^2)
q_l	outlet flux(m^3/m^2)
s_c	average mass fraction of solids in the cake
s	mass fraction of solids in slurry
t	time (s)
w	mass of dry solids per unit area (kg/m^2)
x	distance opposite of flow direction started on filtration screen (m)
A	superficial pad area normal to the direction of flow (m^2)
C	concentration of fiber suspension or fiber pad (kg/m^3)
C_m	fiber mass fraction
C_v	fiber volume fraction
C_0	fiber concentration in the slurry (kg/m^3)
C_{avg}	average fiber concentration in the mat (kg/m^3)
C_{60}	average mat fiber concentration at 60 seconds (kg/m^3)
K	permeability of pulp pad
L	pad thickness (m)
P_s	mechanical pressure in Pa
Q	volumetric flow rate (m^3/s)
R	filtration resistance, m^{-1}
S_0	surface area per unit volume of solids (m^2/m^3)
V	filtrate volume (m^3)
α	specific swollen volume (m^3/kg oven dry fiber)
β	Empirical constants in equation 4-10, 11
δ	Empirical constants in equation 4-10, 11
ε	porosity of the bed
ε_s	cake solidosity (volume fraction of cake occupied by solid)
ε_s^0	Empirical constants in equation 4-10, 11
γ	1.0 m^3/kg in equation 3-6
κ_0	Empirical constants in equation 4-10, 11
μ	fluid dynamic viscosity (Pa.s)
θ_l	volume fraction of swollen fiber, at a fiber concentration of 1.0 kg/m^3
ρ	density of the filtrate (kg/m^3)
σ	specific external surface area (m^2/kg oven dry fiber)

ΔP	pressure drop across the pad (Pa)

CHAPTER 1

INTRODUCTION

Pulp and paper is Canada's largest industry and employer. Kraft pulp is the second largest export of Canada. In Kraft pulping, the pulp washer process is an important unit operation. Better washing with limited water usage is the objective for every pulp mill. For a rotary vacuum drum pulp washing process, each washing stage includes a head-box, vat, rotary vacuum and filtrate (see Figure 1-1). The slurry from the screens or the pad discharge from the previous washer is fed into a head-box. In the head-box, fiber is diluted to between 1 and 2 % consistency with filtrate from the filtrate tank of the washing stage. The slurry then flows over a weir into the vat. The vacuum drum rotates through the vat and accumulates fiber on the drum wire. Increased vat consistencies and vat levels allow more fiber to accumulate on the drum wire at a set rotation speed. Adequate vat dilution results in a better formed, better draining mat (Kempe, 1995). The pulp sheet formation, growth and washing processes on the drum wire can be divided into four zones: sheet formation, displacement washing de-watering, and discharge.

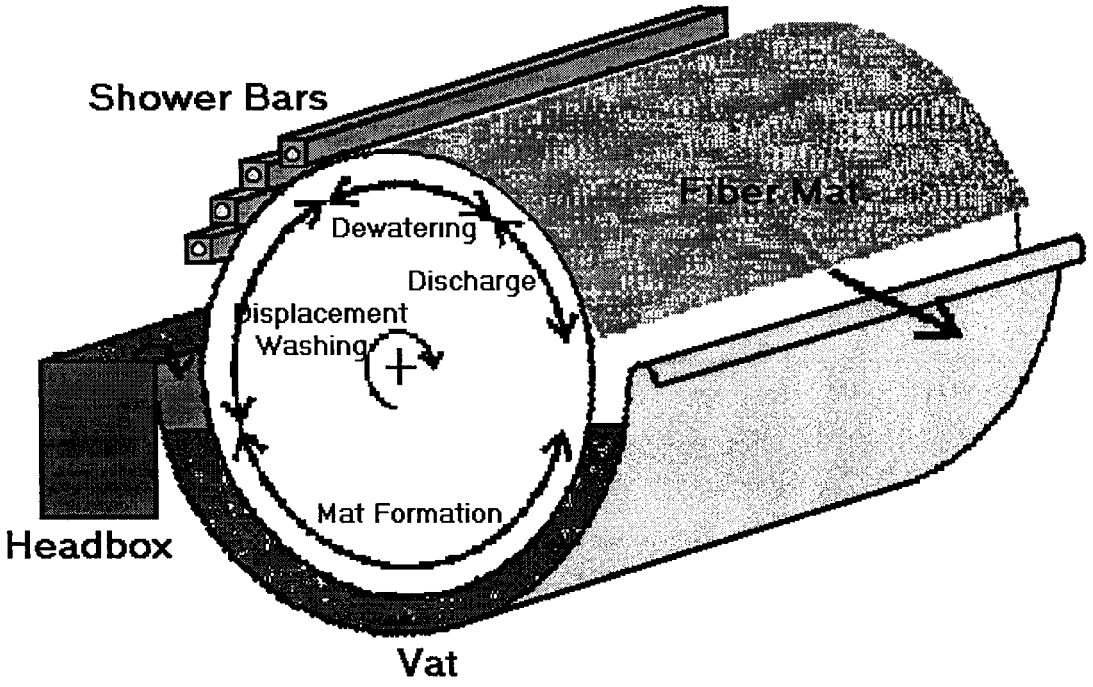

Figure 1-1 Schematic drawing of industrial rotary vacuum washer (Kempe, 1995)

In this operation a large (~ 10 m long, ~4 m diameter) screened drum is partially immersed into a vat containing 1% wt wood pulp fibers (see Figure 1-1) in aqueous pulping liquor. A vacuum is applied to the inside of the drum causing liquor to flow through the screen and subsequent build up of a fiber pad on the drum surface. The drum rotates at about 4 RPM causing an approximately 40 mm thick fiber pad on the drum screen surface to emerge from the vat. Water is sprayed onto the fiber pad after withdrawal from the vat to displace the liquor from the fiber pad. The pad is scraped from the drum surface just before the screen re-enters the vat.

In Kraft pulping, brownstock pulp washing is the cornerstone. Because better washing results in better chemical recovery, less bleaching chemical usage and less waste chemicals discharge to the environment. More wash water used in washing results in cleaner pulp. Due to the energy consumed in evaporation for chemical recovery, the use of too much water usage is expensive and inefficient. In order to maintain higher washing efficiency and furthermore to improve it, it is necessary to understand the influence of all the related key parameters. A mechanistic mathematical model, based on experiments, can be used to process optimization and control. That will make it possible to further improve the process efficiency.

1.1 REVIEW OF PULP SUSPENSION FLOW AND MAT FORMATION

Fiber suspension flow exhibits non-Newtonian flow behavior as shear-rate dependent viscosities and normal stress differences, large elongational viscosities, and yield stresses, even when the suspending fluid is Newtonian. Fibers in these suspensions commonly entangle to form flocs, producing uneven fiber mass distributions in the suspensions. It is very important to understand how macroscopic properties (suspension rheology) and fiber mass distribution are influenced by suspension conditions, particle concentration, suspending fluid viscosity and flow geometry as well as the effects of fiber features such as fiber shape, flexibility and surface roughness.

For a macroscopic (continuous) approach for a pulp suspension, most of contributions in this area are from Kerekes (1995) and his research group by measuring the average floc size, D, using an image-analysis system. An erosion/dilation technique

was used to differentiate joined and overlapping flocs. The average floc size was determined from the measured number and perimeter of flocs. Two parameters were used to quantify the characteristics of uniformity, contrast intensity and a specific perimeter. The contrast intensity measures the variance of image brightness, the "grain" of the texture of the image. Thus dense, large flocs would yield a large contrast intensity and small specific perimeter. A floc is defined as a zone darker than a pre-defined threshold level, which is determined from the mean value of transmitted light. Bubble size measurement in a quiescent fiber suspension at varied mass consistency was reported by Heindel (1999) who employed flash X-ray radiography. We can use these two experimental methods to quantify the size of flocs and bubbles.

The presence of a yield stress of the pulp suspension is one of the main characteristics that affects the observed macroscopic properties of fiber suspension flow. Bennington (1991) indicated that pulp fiber suspensions containing up to 12% fibers by mass were shown to display fluid-like behavior characteristic of yield bearing fluids. The yield stress of commercial wood pulp suspensions at low and medium mass consistency have values typically in the range of $C_m = 0.005$ to 0.35 (C_m is fiber mass fraction, Bennington et al., 1990). An empirical power law model was employed to correlate the yield stress with volume fraction of pulp fibers, $\tau_y = aC_v^b$ (a, b are constant and C_v is the pulp fiber volume fraction). Zhao and Kerekes (1993) found that the uniformity has been shown improved dramatically in wood fibers suspension in a liquid of increasing shear and reaching levels of near perfect uniformity at concentrations in which water alone would yield gross flocculation.

For the microscopic (particle-based) approach, the pioneer of particle-level models was Jeffery (1922). He derived the equation for the motion of an ellipsoidal particle in Stokes flow of a Newtonian fluid. In recent years, computer simulations have been carried out for the dynamics of particles in these suspensions. Brady and Bossis (1985) proposed the Stokesian dynamics method that accurately dealt with hydrodynamic interactions between the particles in the suspension. Yamamoto et al. (1993, 1994, 1995) proposed a dynamic simulation for rigid and flexible fibers in a flow field. The fiber is regarded as made up of spheres, which are lined up and bonded to each neighbor with springs. Each pair of bonded spheres can stretch, bend and twist by changing bond distance, bond angle and torsion angle between spheres, respectively. The authors claimed their simulation results could reproduce the dynamic behavior of rigid and flexible fibers in a flow field, with comparison to the experimental work of Forgacs and Mason (1959). Adopting the method from Yamamoto and Matsuoka (1993, 1994, 1995), Ross and Klingenberg (1998) have recently developed a particle-level simulation technique, fibers are modeled as chains of prolate spheroids, connected through ball and socket joints. The authors claimed that their simulation method qualitatively reproduces known behavior of both rigid and flexible fibers. Ross also claimed that Yamamoto's model could be only used for small aspect ratio (< 10) fibers. The disadvantage of Yamamoto's model has been eliminated in Ross model.

The microscopic approaches are fundamental but further away from complex system applications because of the usage of relatively dilute solutions, limited fiber-fiber contact and relatively small volumes. The macroscopic, or pseudo-continuum approach,

though lacking in detail at the fiber level, allows flow predictions by assuming reasonable averaging over local volumes or layers in the mat formation process. Basically the present research approach is a macroscopic perspective, to facilitate industrial applications.

1.2 REVIEW OF PULP FORMATION MODELS

Pulp mat formation essentially is a filtration process. Modern research of cake filtration started with the classical work of Ruth et al (1933), who found the initial filtration cake to be hard and dry and could be considered as incompressible materials. The thickness of this initial cake could be several millimeters. He also found that the initial cake formation behavior differed from its behavior in the later stages of filtration. Tiller (1960) and his associates have studied cake filtration for the last four decades, and most modern filtration principles and concepts come from their work. Although the detailed solution was not given, Tiller and Cooper (1960) were the first to use non-linear partial differential equations, which were based on the porosity change and the flow velocity variation, to describe the filtration process. A numerical solution of the non-linear partial differential equation in Tiller and Cooper (1960) was reported by Shirato (1969). However, there is no experimental data to support their numerical calculations, so the validity of their work is yet to be tested. Smiles (1970) proposed a different numerical model, which did not use commonly accepted filtration terminology, making it conceptually difficult to understand, and he also used inappropriate boundary conditions. This model can be only used in very limited cases. The moving surface of the growing cake was first formulated as a Stefan problem by Atsumi and Akiyama (1975), with

satisfactory agreement with experimental data. An approximate numerical solution, based on continuity and Darcy's law with an imposed porosity profile, was proposed by Wakeman (1978). He assumed the cake solid volume fraction at the cake/medium interface remains constant during filtration. Stamatakis and Tien (1990, 1991) adopted most of the filtration concepts and principles presented by Tiller and his associates and took the boundary treatment from Atsumi and Akiyama (1975), they provide a method of numerical solution of the cake formation and growth problem; however, there were a number of questions left open in the work. Tien (1997) proposed another model to consider the moving boundary nature of the cake formation process with fine particle retention.

Based on Darcy's law and a mass balance, Jonsson and Jonsson (1992) proposed a dynamic model of water flow during wet pressing. In this paper, they assumed "There is no mixing of solid material between different layers in the solid matrix, the amount of solid, Δm_s is the same in each element Δy; $\Delta m_s = WA\Delta y$ ". Where Δy is relative thickness of fiber mat defined by the authors, W is the basis weight and A is the cross-sectional area of the medium, both constants. Although their complicated numerical solution (Taylor series expansion for local linearization) can be further simplified (see chapter 5 of this thesis), it is a good description of wet pressing, which is different from our mat formation process.

There are many other publications describing the pulp washing process and pulp mat or paper properties. Models vary from the simplified steady-state Norden (1966) efficiency model to detailed mechanistic models. The concept of a Norden efficiency

factor was derived by comparing a real washing system to a hypothetical system comprising a series of countercurrent ideal dilution-thickening stages. Norden efficiency is a steady state concept representing the long-term performance of an actual washing system; it has been extensively used by industrial design. Zahrai (1998) and Martinez et al (1998) proposed a 2-D cross-flow filtration cake formation model for dewatering in a fixed curved channel that compared the power-law type model with their fluid-like model. Numerical simulations were carried out in which differences between the wall and the inlet suspension speeds were varied. They claimed their fluid-like model is more sensitive to this speed difference than that of the commonly used power law model. Their work was focused on dewatering part of pulp washing rather than mat formation under the vat. Permeability and porosity models of a two-dimensional network of cellulose fibers were proposed by Nilsson and Stenstrom (1996). Sampson et al (1995) predicted permeability of pulp fiber mat with Nilsson and Stenstrom's model and the results were compared with Kozeny-Carman theory. Jackson (1986) presented an extensive literature search of experiments and theories related to low-Reynolds number flow through fibrous porous media. Zhu et al. (1995) proposed a mechanistic model to describe fluid permeation through compressible fiber beds based on the micro-mechanical theories of compressibility of fiber assemblies from textile science and engineering. The simulation of multi-permeability porous media and its interface effect were reported by Lappan, Hrymak and Pelton (1997). Dodson (1996, 1997), Deng (1994) and Scharcanski (1996) used the theory of texture image analysis to obtain a new method for the evaluation of anisotropy in planar stochastic structures. The authors claimed their model could be

applied in the forming of non-woven textiles and paper from fiber suspensions and in modeling void structures and transmission of fluids.

It is very important for the industrial process not only to predict process performance, but also to analyze the process on a rational basis with the understanding of the mechanisms involved and to account for all of its parameters. A model that is developed correctly can be used to assess the relative effects of the various mechanisms and determine the sensitivity to changes in the model parameters. It can, therefore, be utilized for process design and optimization. However there is no such a model available in the literature for the pulp washing process.

1.3 FUNDAMENTALS OF BUBBLE BEHAVIOR AND CHANNELING

In brownstock washing, defoamers are continuously added to alleviate the adverse effects of dispersed air - without defoamer addition washer throughput is too low. Recently, there have been many attempts to characterize the hydrodynamics of pulp suspensions and bubble behavior of water-fiber-air three-phase system in flotation deinking of waste paper and gaseous fiber bleaching processes. Reese et al. (1996) indicated that the hydrodynamic behavior of a three-phase pulp slurry is significantly different than air bubbles in pure water, even at very low pulp consistencies. The presence of pulp in the column leads to bubble coalescence, which increases the average bubble size and reduces the overall gas hold up. Pelton and Piette (1992) found that bubbles streams bypass flocs or coalesce into larger bubbles with enough buoyant force to break through the fiber network. In a study of bubble behavior in a quiescent liquid column and a concurrent air-liquid and column, Lindsay et al. (1995) stated that the

models and correlations based on nonfibrous data cannot be applied to the water -fiber system because of the effect of the fiber network. Observations of air bubble dynamics have been done by X-ray analysis (Heindel and Monefeldt, 1998). The effect of fiber consistency on bubble size (Heindel and Garner, 1999), and the effect of pulp fibers on gas holdup in a flotation column (Janse et al., 1999) have been reported.

All of the above mentioned publications correspond to systems in flotation deinking of waste paper or gaseous fiber bleaching, which can be thought of as a three-phase fluidization operation (Reese et al, 1996). For rotary pulp washing, it is more like a filtration, because there is a pressure drop, typically 15 to 30 kPa, across the wire mesh and fiber pad on the drum's surface . This pressure gradient is the driving force for the filtration of liquor through the pad. The filtration of vat liquor results in the accumulation of fiber on the drum surface and the pad grows. However there is a significant air bubble presence in this operation and air bubbles play very important roles in the water flux through the pad, the effects of air bubble behavior in pulp washing processes have not been studied by many researchers.

The objectives of Chapter 2 are: to observe bubble behavior in the pulp mat formation process, to understand how channels are formed, and to determine the mechanism by which bubbles and channel effects contribute to pad heterogeneity in the filtration process.

1.4 THE SCOPE OF THIS THESIS

Chapter 2 addresses the bubble behavior and effects in mat formation. Chapter 3 presents a new pulp mat permeability model, which can be applied over a wide range of fiber concentration. Chapter 4 provides experimental measurements of mat formation and a model based on traditional filtration theory. Chapter 5 describes a novel model formulation and numerical solution for pulp mat formation from dilute pulp suspensions. Chapter 6 presents the major conclusions of the thesis work.

REFERENCES

ATSUMI, K and AKIYAMA, T "A Study of Cake Filtration", *J. of Chem Eng. of Japan,* Vol. 8, No. 6 (1975)

BENNINGTON, C. P. J. and KEREKES, R. J. and GRACE, J. R. "The yield stress of fiber suspensions" *The Can. J. of Chem. Engr.* Vol. 68, Oct. (1990)

BRADY, J. F. and BOSSIS, G., *J. Fluid. Mech.* 155, 105 (1985)

DENG, M. and DODSON, C. T. J, "Random Star Patterns and paper formation" *Tappi* Vol. 77. No. 3 pp. 195-199, March (1994)

DODSON, C. T. J. and SAMPSON, W. W., "Modeling a class of Stochastic Porous Media" , *Appl. Math. Lett.* Vol. 10, No. 2 pp87-89 (1997)

DODSON, C. T. J. "Fiber crowding, fiber contacts and fiber flocculation" *Tappi* Vol. 79, No. 9 pp211-216 Sept. (1996)

FORGACS, O. L. and MASON, S. G., *J. Colloid Sci.* 14, 473, (1959)

HEINDEL, T. J. "Bubble size measurements in a quiescent fiber suspension" *J. Pulp Paper Sci.* Vol. 25 No. 3., March (1999)

HEINDEL, T. J. and GARNER, A. E., "The effect of fiber consistency on bubble size" *Nordic Pulp Paper Res. J.* Vol. 14 No. 2, (1999)

HEINDEL, T. J. and MONEFELDT, J. L. "Observations of the bubble dynamics in a pulp suspension using flash X-ray radiography" Vol.81 No. 11 *Tappi* (1998)

JACKSON, G. W. "The permeability of Fibrous Porous Media" *Can. J. of Chem. Eng.* Vol.64, June pp.364, (1986)

JANSE, P.; GOMEZ, C.O. and FINCH, J. A., "Effect of Pulp Fibers on Gas Holdup in a Flotation Column", *Can. J. Chem. Eng.* Vol.77 (1999)

JEFFERY, G. B., *Proc. R. Soc.* London, Ser. A 102, 161 (1922)

JONSSON, K. A. and JONSSON, B. T. L. "Fluid Flow in Compressible Porous Media, dynamic behavior" *AIChE J.* Vol. 38 No. 9 pp.1349-1356 (1992)

KEMPE, M. J., "Dynamic Modeling of a Vacuum drum washing system" Master's thesis Chemical Engineering Department, McMaster University (1995)

LAPPAN, R. E. and HRYMAK, A. N. "Dependence of in situ precipitate deposition on flow characteristics in multi-permeability porous media" *Chem. Eng. Sci.* Vol.52 No. 17 pp2963-2975, (1997)

LINDSAY, J. D.; GHIAASIAAN, S. M. and ABDEL-KHALIK, S. I. "Macroscopic Flow Structures in a Bubbling Paper Pulp-Water Slurry" *Ind. Eng. Chem. Res.*, 34, 3342-3354, (1995)

MARTINEZ, D. M. "Characterizing the Dewatering Rate in Roll Gap Formers" *J. Pulp and Paper Sci.* Vol. 24, No. 1, January (1998)

NILSSON, L. and STENSTROM, S."A Study of the permeability of Pulp and Paper" *Int. J. Multiphase Flow* Vol. 23 No. 1 pp131-153, (1997)

NORDEN, H. V. "Analysis of a Pulp Washing Filter", *Kem. Teollisuus* 23, 343-347 (1966)

PELTON, R. H. Polymer-Colloid Interactions in Pulp and Paper Manufacture, Colloid-Polymer Interactions from Fundamentals to Practice Edited by Raymond S. Farinato and Paul L. Dubin John Wiley & Sons , Inc. (1999)

REESE, J. P.; JIANG and FAN, L.-S "Bubble Characteristics in three-phase systems used for pulp and paper processing" *Chem. Eng. Sci* Vol. 51 No. 10 pp.2501-2510, (1996)

ROSS, R. F. and KLINGENBERG, D. J., *J. Pulp and Paper Sci.* Vol. 24 No. 12 Dec. (1998)

RUTH ,"Studies in Filtration" *Ind. Eng. Chem.*, 25, 76, 153, (1933)

SAMPSON, W. W. and BRIDLE, I. J. "Simulation of the directional dependence of flow through fiber mats" *Nordic Pulp and Paper Res. J.* No. 2, pp. 145-149, (1995)

SCHARCANSKI, J. and DODSON, C. T. J. "Texture analysis for estimating spatial variability and anisotropy in planar stochastic structures" *Opt. Eng.* 35(8) 2302-2309 August (1996)

SHIRATO, M. *et. al* "Internal Flow Mechanism in Filter Cakes" *AIChE J.* Vol. 15, No. 3 pp405-409, (1969)

SMILES, D. E. "A theory of constant pressure filtration" *Chem Eng Sci* Vol. 25 pp985-996 (1970)

STAMATAKIS, K and TIEN, C. "Cake formation and growth in cake filtration" *Chem Eng Sci* Vol. 46 No. 8 pp1917-1933 (1991)

TIEN, C. , BAI, R. and RAMARAO, B. V. "Analysis of Cake Growth in Cake Filtration: Effect of fine particle retention" *AIChE J.* Vol. 43, No. 1 pp.33-44 (1997)

TILLER, F. M. and COOPER, H. R., "The Role of Porosity in Filtration: IV. Constant Pressure Filtration" *AIChE J.*, 6, 595, (1960)

WAKEMAN, R. J. "A numerical integration of the differential equations describing the formation of and flow in compressible filter cakes" *Trans I Chem E.* Vol. 56, (1978)

YAMAMOTO, S. and MATSUOKA, T."A method for dynamic simulation of rigid and flexible fibers in a flow field" *J. Chem. Phys.* 98(1), January (1993)

YAMAMOTO, S. and MATSUOKA, T ,"Viscosity of dilute suspensions of rodlike particles: A numerical simulation method" *J. Chem. Phys.* 100(4), 15 Feb. (1994)

YAMAMOTO, S. and MATSUOKA, T. "Dynamic simulation for fiber suspension in shear flow" *J. Chem. Phys.* 102(5), February (1995)

ZAHRAI, S. F.; BARK, H. and MARTINEZ, D. M."A numerical Study of Cake Formation in 2-D cross-flow filtration" *J Pulp and Paper Sci.*: Vol. 24 No.9 September pp 281-285, (1998)

ZHAO, R. H. and KEREKES, R. J. "The effect of suspending liquid viscosity on fiber flocculation" *Tappi* Vol. 76, No. 2, (1993)

ZHU, S.; PELTON, R. H. and COLLVER, K. "Mechanistic Modeling of Fluid permeation through compressible fiber beds", *Chem Eng Sci* Vol. 50, No. 22 pp3557-3572, (1995)

CHAPTER 2

NEW INSIGHTS INTO DISPERSED AIR EFFECTS IN BROWNSTOCK WASHING

SUMMARY:

A laboratory washing cell was used to visualize pad formation on the surface of a simulated brownstock washer drum submerged in a washer vat. Large dispersed air bubbles (diameter > 10 mm), obtained in the presence of defoamer or the absence of black liquor, passed through the fiber pad having little influence on the water flux. By contrast, small bubbles (< 2mm) were trapped in the pad, lowering filtration fluxes by as much as a factor of 100. The detrimental effects of small bubbles on drainage were diminished by defoamer addition, which caused the little bubbles to coalesce and to escape through the pad.

The passage of large bubbles through the growing pulp pad appeared to produce channels. It is possible that the channels may explain poor displacement washing efficiencies reported for some washers.

2.1 INTRODUCTION

Brownstock washing is a key unit operation in the production of kraft pulp, affecting the efficiencies of both bleaching and the recovery cycles. Our interest in washing is focused on the effects of dispersed air, which is known to interfere with

washing (Dougherty, 1989 and Pelton 1989). Excessive air can influence washing efficiency in at least two ways. First, foam buildup in the drop leg decreases the drum vacuum that is the driving force for water flow through the pulp pad (Browne and Perrault, 1978). Second, in flowing pulp suspensions air bubbles present in the vat lower water drainage rates through pulp pads (May and Buckman, 1975). The paper technology literature provides no information about the relative importance of these mechanisms. This work focuses on the effects of dispersed air in the washer vat on the formation and drainage properties of the pulp pad, which in turn influence washer productivity (Crotogino et al., 1987). Air bubbles are generated in the normal processing of wood pulp suspensions, especially in a rotary drum washer. Fibers isolate dispersed bubbles from each other giving a reduced opportunity for bubble-bubble collisions that can cause the bubbles to coalesce to larger bubbles. The fibers also inhibit bubble rise and escape to the headspace. Piette and Pelton (1992) showed that in quiescent pulp suspensions, small bubbles could not break through the network of fibers flocs to reach the surface. In flowing pulp, where fiber network structures are more transient, bubble rise is somewhat easier (Isler and Widmer, 1979). The overall effect is that it is relatively easy to sustain a dispersed air content of four volume percent in a 1% consistency pulp whereas in water this air would rise to the surface either to give foam or to dissipate into the headspace.

Brecht and Kirchner (1961) reported that drainage rates in a handsheet machine were significantly lower when dispersed air was present. This observation has been verified in more recent work (Karras and Springer, 1989); however, there is little

quantitative information about the effects of air bubble size or concentration on pad permeability. From a practical perspective, the solution to air-related problems is the addition of defoamers.

Brownstock defoamers are continuously added to alleviate the adverse effects of dispersed air. This is critical for most washer operations- without defoamer addition washer throughput is very low. The mechanisms by which defoamers improve pulp pad drainage are not obvious. By contrast, the scientific literature contains many papers (Wang et al., 1999; Garrett, 1993) describing how defoamers prevent foam formation. The details are beyond the present scope- the key conclusion is that defoamers accelerate the rate of coalescence of neighboring bubbles in foam. In pulp slurries, this means that when two air bubbles collide in flow they have a much higher probability of coalescing to form a single, larger bubble in the presence of defoamer. Why should this give better washer operation? An obvious explanation is that if defoamer is added before pulp washing, the dispersed air bubbles in the pulp will coalesce to give larger bubbles, within the forming pulp pad, that can more easily escape to the headspace. In support of this explanation Dougherty (1989) has shown that defoamer addition dramatically lowers the dispersed air content in the vat and many mills now use dispersed air sensors to control defoamer addition rates. Under normal operating conditions the amount of added defoamer is very low, it did not remove all the dispersed air from pulp suspension before washing and yet washer throughput is improved -could another mechanism be operative?

Herein we report the results of direct observations of the behavior of air during pulp fiber pad formation on the surface of a washer screen. We will show that air can influence both pulp pad structure and permeability. Furthermore, we will show that defoamers prevent small air bubbles from being trapped in the compacted pulp pad adjacent to the screen to interfere with drainage.

2.2 EXPERIMENTS ON MAT FORMATION:

Figure 2-1 shows a schematic diagram of the McMaster laboratory pulp washer, which simulates pulp pad growth on a washer drum screen while submerged in a washer vat. The transparent, poly (methyl methacrylate), filtration cell has dimensions of 200 x 155 x 20 mm (H x W x T). A washer screen forms the top of the cell. A vacuum is applied above the screen causing pulp to enter from below and form a pad by filtration on the underside of the screen. The thin cell is illuminated by transmitted light (Visual Plus, Model VP-4050v) and pad formation is recorded with a digital video camera (Canon ZR 30 frames per second and 720 x 480 pixels) located about 2 m from the cell. The range of bubble diameters was estimated from the video images taken at a higher magnification.

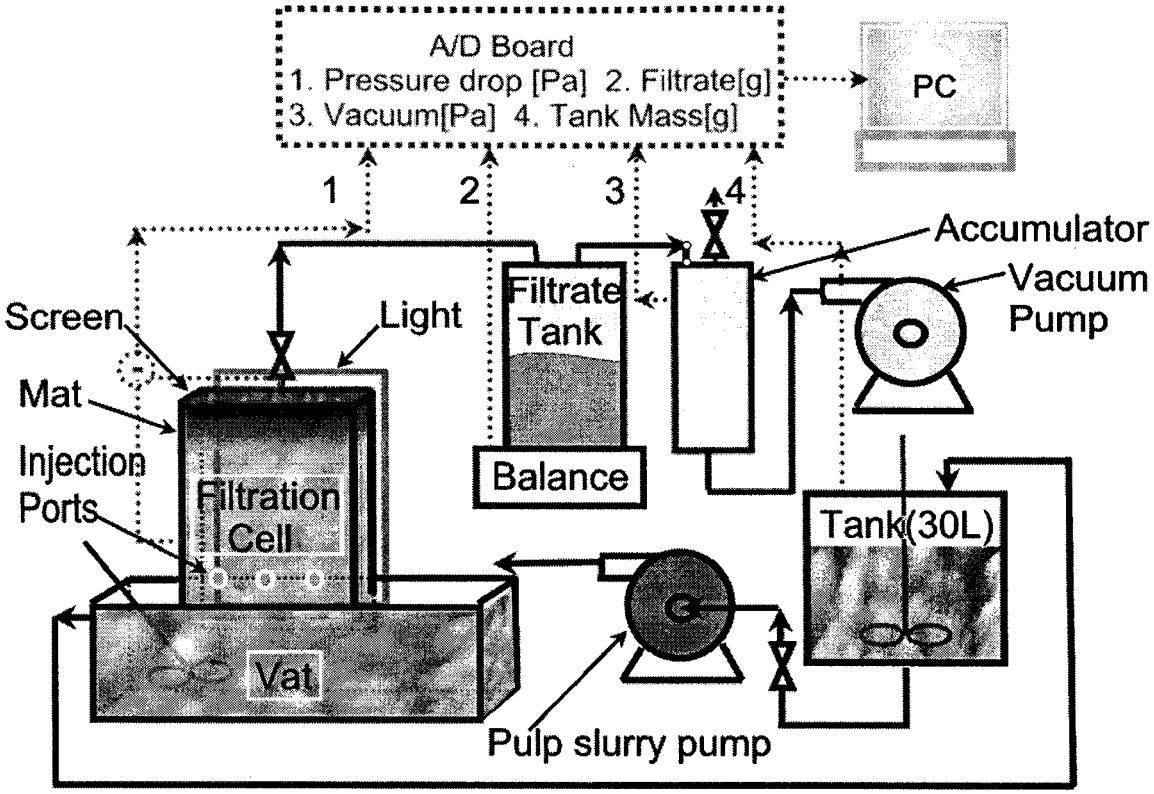

Figure 2-1. Schematic diagram of laboratory pulp filtration apparatus.

A Welch duo-seal vacuum pump (Sargent-Welch Scientific Co. model 1400) coupled to a 9.6 L accumulator was used to generate the vacuum. The accumulator vacuum was measured with a Celesco DP30-0001-111 pressure transducer whose readings were logged on a PC using TESTPOINT™ (Capital Equipment Corporation, version 2.0a 1995) software coupled to a DAS-802 A/D board (Keithley Metrabyte Co.). The accumulator pressure was adjusted manually by an air-bleed valve. The filtrate mass was measured with a digital balance (Mettler PM16) and logged by the PC at a frequency of 1Hz.

A Moyno cavity pump model A1B SS03 AAA was used to circulate pulp between a 30L tank and the 4 L vat. A weir was employed to maintain a constant vat level. In a typical experiment, the tank (see Figure 2-1) is filled with 30 liters of water and 300 gram of air-dry softwood bleached kraft pulp (Avenor, Thunderbay), to give a final consistency of 0.93 %(wt). After turning on the pulp slurry pump and the two mixers, the vacuum pump is turned on and the pressure adjusted manually to the desired value (usually 20.0 kPa or 66.7 kPa). The valve between the filtration cell and the filtrate tank is opened slowly to fill the filtration cell and then fully opened to commence flow through the screen.

In some cases air was injected at a controlled volumetric flow rate through ports on the side of the filtration cell. The flow rate was controlled with a Harvard Apparatus Model 2400-004 syringe pump. The orifice was made of plastic tubing with an inner diameter of about 1.5mm. For some experiments, Palmolive dishwashing liquid was employed to obtain small stable bubbles. For these experiments the pulp recirculation loop was not used because the weir entrained many air bubbles, which can overflow out of the vat. Instead, the vat was filled with 4L of pulp, and up to 0.5g of Palmolive dish washing detergent was added and the vat mixing propeller was used to entrain air.

2.3 RESULTS:

A 1% consistency bleached kraft pulp suspension was used in the laboratory filtration apparatus (Figure 2-1) to visualize pad formation. Upon applying a vacuum, pulp suspension rises from the vat to fill the filtration cell. A pad accumulates below the

screen as water passes up through it. Thus, the apparatus mimics pulp pad formation on the submerged sector of a pulp washer drum.

Four video frames showing the filtration cell (200 mm x 150 mm) during a typical experiment are shown in Figure 2-2. The dark regions correspond to high local fiber concentration whereas the white regions are pure water. At 10 s most of the cell contains flocculated pulp suspension, which is characterized by a mixture of fiber rich and fiber lean (white) domains. Only the top two centimeters are uniformly dark - this is the fiber pad. At longer times the pad continues to grow (down) towards the vat. Note that in a real washer, fiber pad formation stops after approximately 5-10 seconds when the drum rotates out of the vat. After the pulp mat formed (at 20 seconds), a blue dye was injected in the middle port at the bottom of the filtration cell. As shown in Figure 2-3, there was no flow channel in the mat.

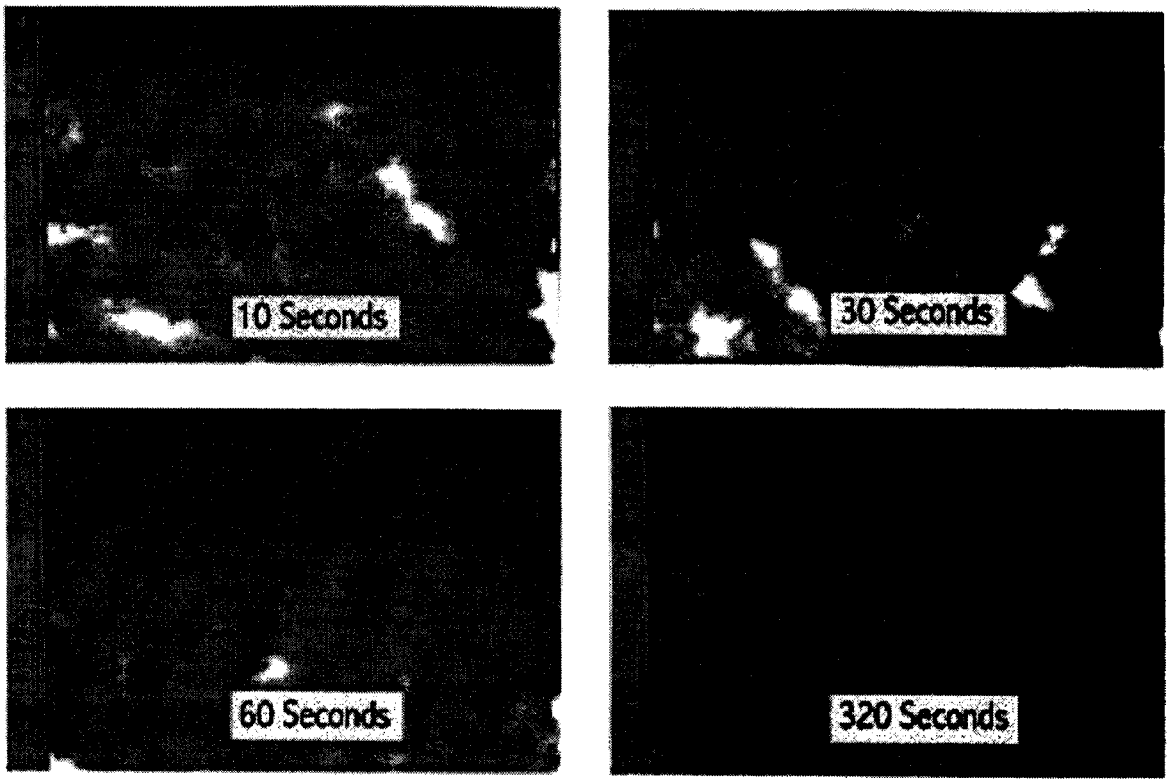

Figure 2-2. **Four frames from a pad formation experiment in which the system vacuum was 20.0 kPa and the suspension contained no added air or surfactant. The white areas are water and the fibers are gray. The scale at the left is centimeters.**

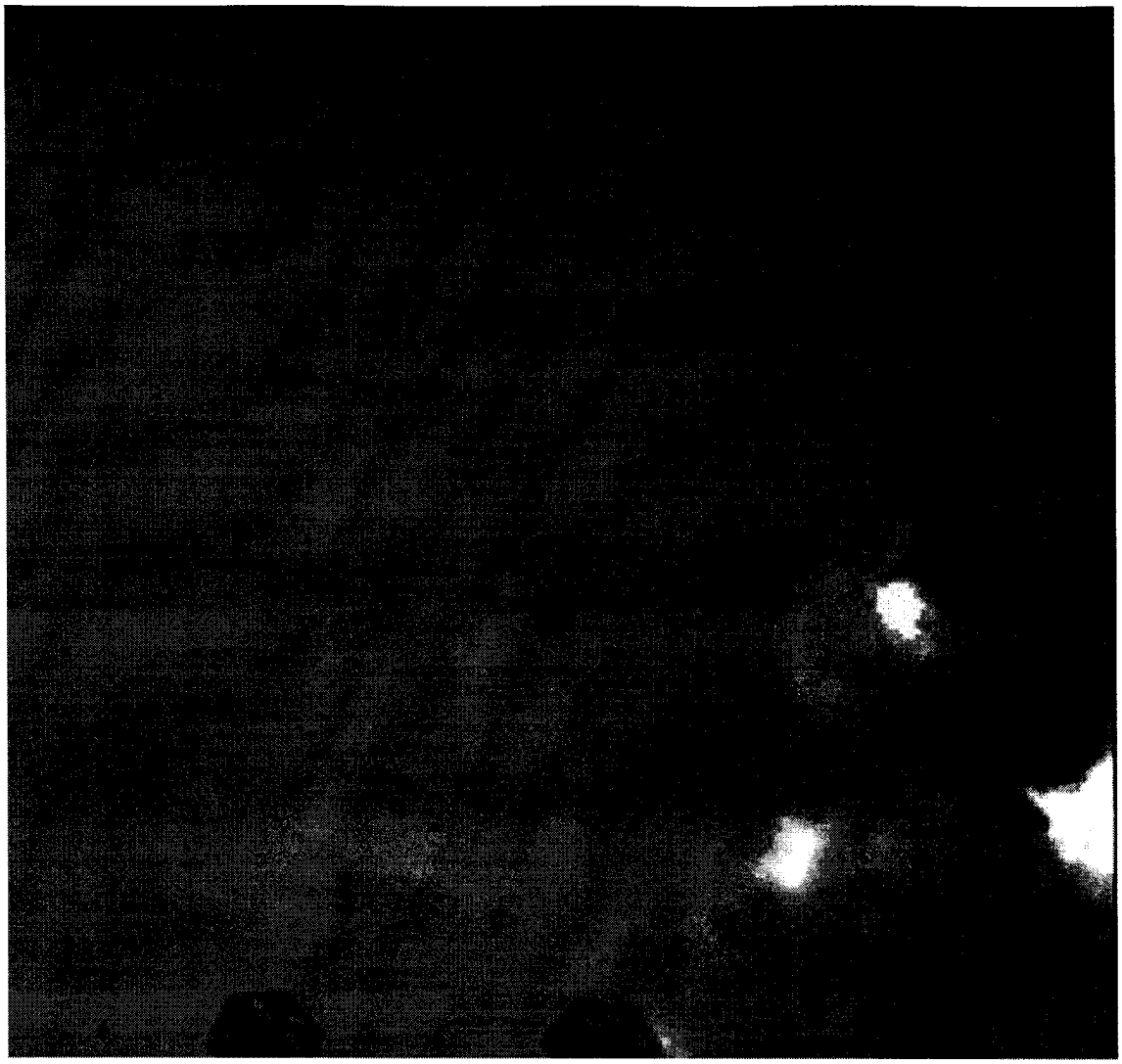

Figure 2-3 Dyed water flow through formed mat

In an attempt to simulate air effects in washing, pad formation experiments were conducted with air injection into one or more ports at the bottom of the filtration cell (see Figure 2-1). Figure 2-4 shows nine frames from a pad formation experiment with air. The paths of the air bubbles are clear when watching the video but are somewhat obscure in single frames. The white solid lines were hand-drawn to highlight the position of the bubble paths, and ellipses, also hand-drawn, indicate the location of trapped bubbles. Air

bubbles rise towards the screen much more rapidly than do the pulp flocs. An initial bubble, like an icebreaker, creates a channel by weaving between the flocs. Subsequent bubbles follow the same path. An example of channel formation is shown in the top center of the 8 and 10 sec frames in Figure 2-4. The tendency for rising bubbles in pulp columns to form channels has been reported by others (Heindel, Monefeldt, 1998; Janse et al. 1999; Lindsay et al. 1995)

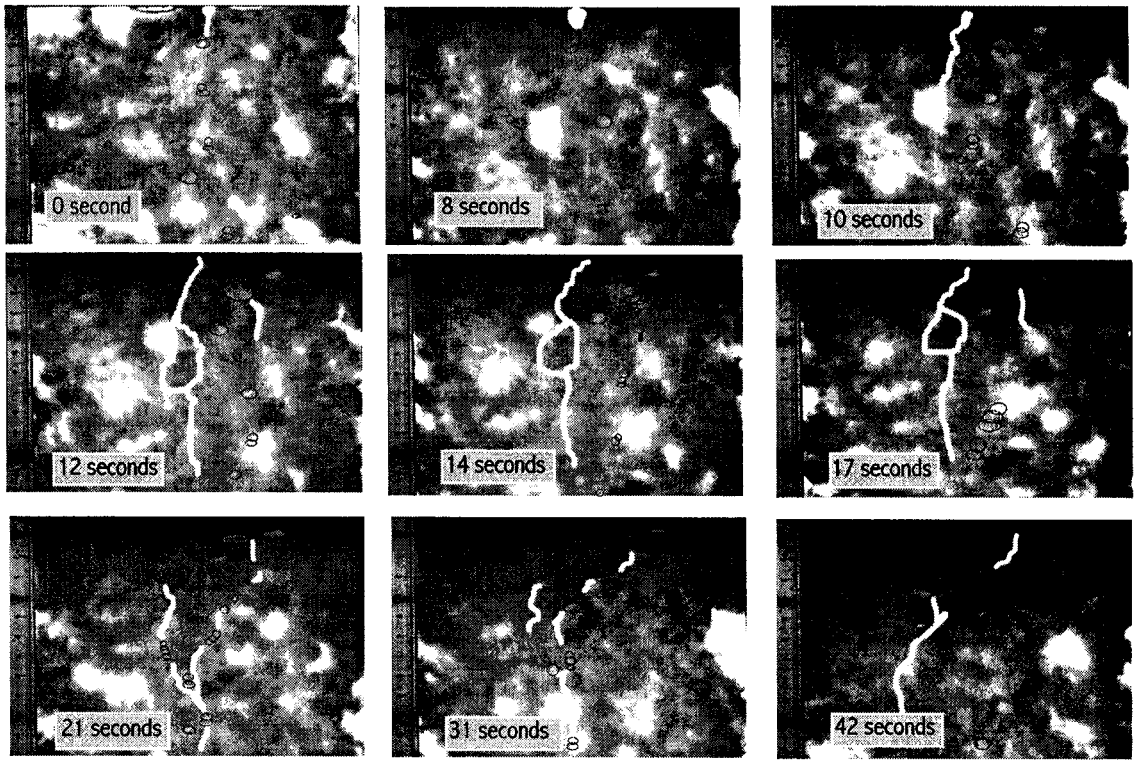

Figure 2-4. Pad formation with injected air (red in picture). White solid lines were hand drawn and indicate the position of channels formed by rising bubbles.

The air that escapes through the pad and wire was visible (but not shown here) in the transparent section above the cell, as very small rising bubbles as if the pad/screen were acting like a fine frit.

Air bubbles in defoamer-free water tended to coalesce upon contact with each other. For example, in Figure 2-4 at 12 seconds the largest ellipse shows the position of a cluster of large bubbles at the end of a channel. Two seconds later the large bubble cluster has grown, having been fed by the stream of small bubbles rising through the channel. However, at 17 seconds, part of the coarse bubble cluster has broken though the pad and screen.

A continuous source of air bubbles seems to be required to maintain a channel. Two channels are highlighted at 21seconds, whereas by 42 seconds the left hand channel has disappeared. Apparently many of the rising bubbles followed the right hand branch after 21 seconds allowing the left hand channel branch to be filled by flowing pulp.

Visible channels seemed to end in the concentrated region of the pad without reaching the screen. The qualitative impression is that many of the air bubbles introduced in this experiment do pass through the pad and screen. Thus, it is possible that a relatively high permeability path continues to the screen and we simply cannot see into the

concentrated mat. Pad compression squeezes the air bubbles near the screen and may remove channels.

Black liquor is very surface active, thus any air bubbles present will not tend to coalesce upon contact each other. In an effort to make the experiments more representative of real washer operation, pad formation experiments were run with the addition of dishwashing detergent, which is a mixture of surfactants with good bubble stabilization properties. With detergent, small bubbles (approximately 2 mm diameter) can collide without coalescing into larger bubbles. Without detergent, the bubbles are much larger and they readily coalesce when pushed together.

In the pad formation experiments with detergent, many small bubbles were trapped in the pulp and they tended not to escape through the pad and the screen. No picture is shown because the bubbles were too small (less than 1 mm) to be seen with our video camera. The presence of small, trapped air bubbles had a dramatic effect on the pad permeability. Figure 2-5 shows the mass of filtrate versus drainage time for a number of experiments. Hundreds of data points were collected for each experiment and the scatter in the data was small so only lines are shown. The curves labeled "water" were for essentially air-free pulp suspension. The drainage rates (the slope of the curves) were decreased as the pulp pad grew. This was classical behavior and, as expected, a higher vacuum gave higher initial drainage rates. The curves labeled "Detergent" were

runs with air and added detergent. The drainage rates were about two orders of magnitude lower with detergent than without indicating that the accumulation of small air bubbles in the pad interfered with water flow.

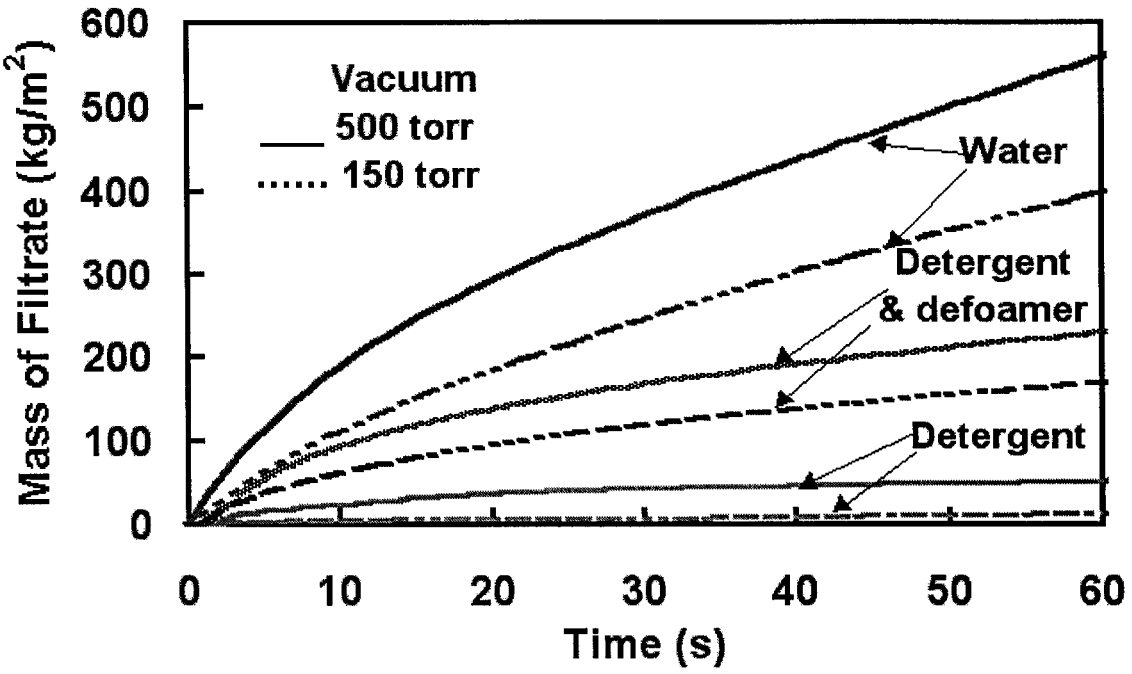

Figure 2-5. The total mass of water drained though the forming pad as a function of drainage time.

Experiments were also conducted with water, air, fibers and a commercial silicone defoamer for brownstock washer provided by Dorset Industrials Chemicals Ltd. The defoamer was added just before pad formation so that the entrained air could not escape. The resulting curves are labeled "Detergent & defoamer" in Figure 2-5. The drainage behavior lay between the other two cases. In other words, air in the presence of defoamer has a reduced detrimental effect on filtrate flow rate, compared with the defoamer-free case.

2.4 DISCUSSION:

Every conventional brownstock washer operator knows that defoamer addition is crucial - without it washer operation in highly surface-active brownstock is impossible. This work shows for the first time that small air bubbles trapped in the pad dramatically reduce flow whereas large bubbles are able to "leak" through the pad and screen and thus have less influence on washing. Thus, the role of defoamers is not only to remove air from stock but more importantly to induce small bubbles to coalesce into large ones which are much more likely to pass through the pad.

In a fundamental study of displacement washing of pulp pads, Crotogino et al (1987) concluded that pads formed on commercial washers are not uniform in comparison with pulp pads carefully formed in a laboratory. They speculated that pad non-uniformity is a consequence of forming pads with flocculated fiber suspensions. In this work we observed channel formation caused and maintained by streams of rising air bubbles, perhaps this is another mechanism for broadening the permeability distribution in pulp pads.

2.5 Bubble behavior in pulp slurry, water and Bingham fluids

The efficiencies of many processes in the pulp and paper industry including pulp washing, bleaching, flotation deinking, and papermaking, depend in part, upon the properties of dispersed gas bubbles in the aqueous wood pulp suspensions. The tendency of suspended particles to retard or to prevent the rise of gas bubbles in water is an area of

considerable study in chemical engineering. Pelton and Piette (1992) have studied the bubble behavior in the still pulp suspension flow. Isler and Widmer (1979) evaluated the tendency of air bubbles to rise through pulp flowing in a horizontal pipe. Schultz and Scott (1991) have also demonstrated in laboratory tests that in the absence of defoamers of vacuum, a fraction of the dispersed air in pulp from a board machine remained in the pulp. Although bubble behavior in compressed pulp mat is one of the keys to understand the mechanism of pulp washing, no report was found in the literature.

2-5-1 Bubble force analysis in three different media

In order to clearly understand the forces involved in trapped bubbles, we provide three hypothetical case studies. In case A, bubbles flow with pure water, so the forces involved in a bubble moving are buoyancy force, drag force and resistance from the screen. The internal bubble pressure is nearly same as the surrounding water. Case B is bubbles flowing in a fluid with a yield stress (Bingham fluid). The forces involved in bubble moving are not only buoyancy force and drag force but also the resisting yield stress. There is yield stress for flow phase in case B, so for small bubbles, the buoyancy force is small enough then the bubble will stay in the fluids. In the compressed pulp mat, case C, all the forces observed in cases A and B are also present.

The pulp mat is porous and inhomogeneous, so small bubbles tend to stay in pores without getting compressed, while large bubbles are compressed by surrounding pulp fibers (see Figure 2-6). There are non-uniform mechanical compression forces involved in bubble movement in case C. This mechanical compression force can be very

large compared with all the forces involved in cases A and B (for a bubble with 10 mm dimension near the filtration screen under 20.0 kPa vacuum, the mechanical pressure on fiber flocs is 20.0 kPa and the mechanical pressure of air bubble near the screen is also about 20.0 kPa, the buoyancy force of the air bubble equals ($1000 kg/m^3 * g * 4/3 \pi * r^3 =$) 0.00513 N, the cross section area of the bubble is $7.854 * 10^{-5} m^2$, so the pressure on the air bubble by buoyancy force is 65.31 Pa. The mechanical pressure on the air bubble is about 310 times of that of buoyancy force . If a big bubble is near the filtration screen, the mechanical compression force will be near the total system vacuum (for vacuum filtration). The small bubbles (staying in pores) have no mechanical force on them by surrounding pulp flocs. Buoyancy and drag forces for these small bubbles are very small while comparing the mechanical force. When defoamer is present, the defoamer induces coalescence which makes it more likely for air to be removed through existing channels rather than being trapped in between the pulp flocs.

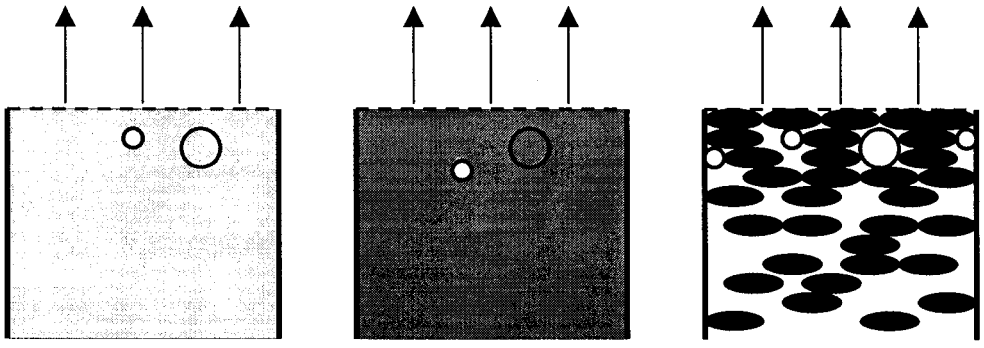

Case A (Water) **Case B (Bingham Fluid)** **Case C (Pulp Slurry, ⬬)**

Figure 2-6 Small bubbles tends to stay in structure of pulp slurry

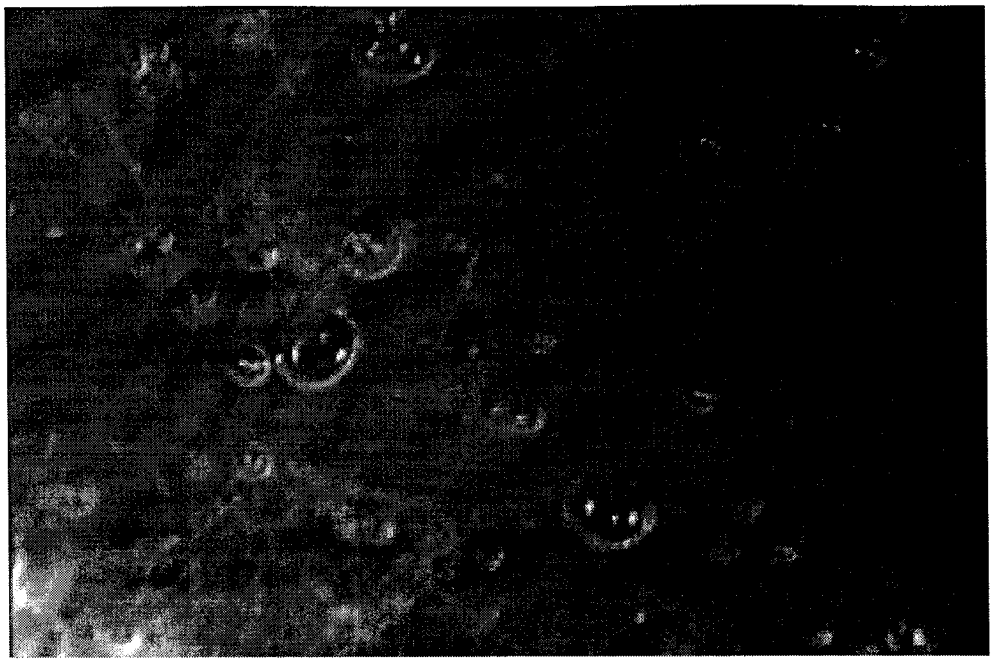

Figure 2-7 Bubbles trapped in pulp fiber flocs (black liquid without defoamer)

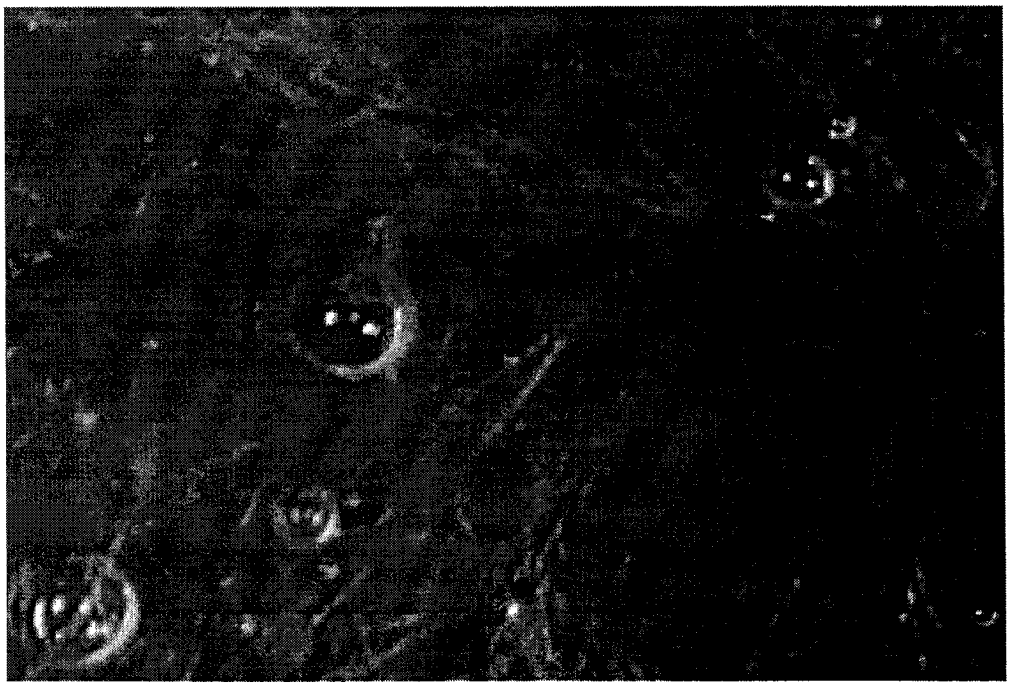

Figure 2-8 Bubbles trapped in pulp fiber flocs (black liquid with defoamer)

Figure 2-7 is an image taken by microscope , which represents an area of 2.0mm x 3.5 mm area. Surfactants in the model black liquor prevent bubble coalescence when two bubbles touch. If defoamer is added, the bubbles will coalesce to form larger bubbles. Large bubbles will either escape out of pulp slurry before entering the washer or get out through the mat, so fewer bubbles will be found in the image (see Figure 2-8). Small bubbles either coalesce to form big bubbles or remain trapped in fiber flocs.

Figure 2-9 shows that a big bubble was surrounded by compressed pulp flocs. It is in a dynamic force balance state, which means that the air pressure in the air bubble and mechanical compressive forces on it are in equilibrium. If there is any weakness in the compressed pulp flocs, the air bubble will move through that weakness.

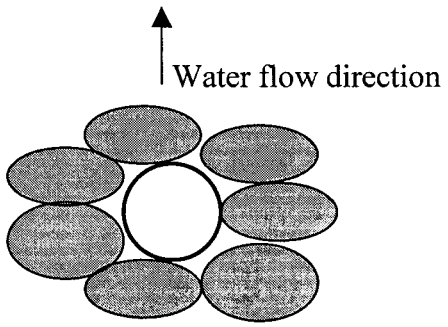

Figure 2-9 Large bubbles tend to be squeezed out by surrounding compressed pulp fiber flocs

2-5-2 Mechanical pressure measurements and yield stress of pulp mat

The compressibility of our Northern Canadian bleached softwood Kraft pulp fiber has been measured. The curve of mechanical pressure and fiber consistency was very close to that measured by Bennington et al (1990) for yield stress and fiber consistency (see Figure 2-10). Yield stress, measured by concentric cylinder, and mechanical pressure measured in compressible experiment are the same.

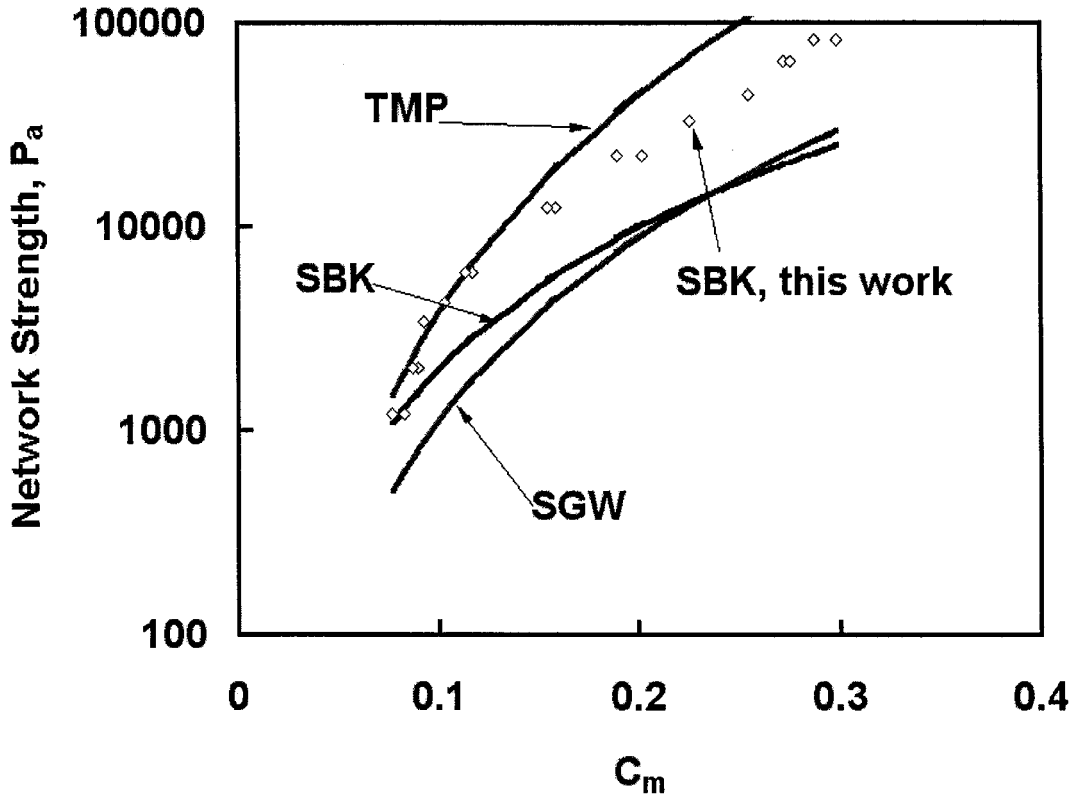

Figure 2-10 Bennington's yield stress of TMP, SBK, SGW and the compressibility of the SBK used in these experiments.

2-5-3 Design of future model experiment on permeability of fiber mat

For the study of the effects of bubble size and pore size in the mat on permeability or mat formation process a simple experiment was designed. Hollow rubber balls filled with water represent fiber flocs. Hollow rubber balls filled with air represent air bubbles. The pore size can be determined by size of rubber balls (filled with water). We can get a series of data to represent the relationship between permeability and the sizes of water balls and air balls.

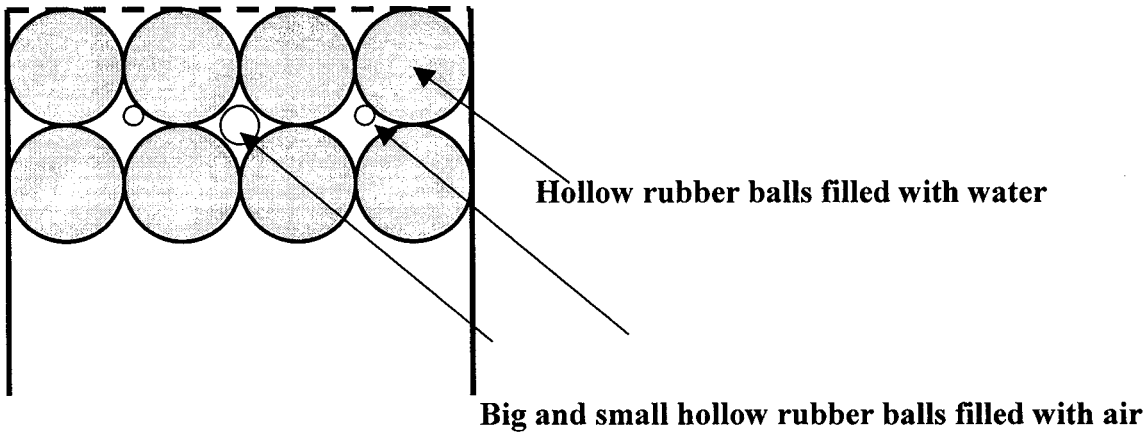

Figure 2-11 Permeability experiment with varied pore sizes and bubble sizes

The main conclusions under our experimental conditions are:

Large bubbles (> 10 mm) flow through the forming pad and the washer screen whereas

-small bubbles (< 2 mm) remain trapped in the pad on our model washer cell. The small bubbles tend to stay in the pores of fiber flocs structures. .

1. Rising air bubbles form channels through the pulp pad during pad formation in the washer vat.

2. Channels appear to end as they approach the high consistency region near the screen.

3. Channels formed at early stages disperse without a steady stream to give a stream of very small bubbles downstream of the screen.

4. Large bubbles near the screen "leak" through the pad and screen to give a stream of very small bubbles downstream of the screen.

5. Trapped air bubbles dramatically reduce mat permeability.

The role of defoamers is to aid the coalescence of small bubbles into larger bubbles, which can escape through the fiber pad, reducing the interference with washing.

REFERENCES:

BRECHT, W and KIRCHNER, U., *Das Papier* 15, 625 (1961)

BROWNE, P and PERRAULT, R. R., *Tappi*, 61(3) 83 (1978)

CROTOGINO, R. H. AND POIRIER, N. A. and TRINH, D. T., *Tappi*, 70(6) 95 (1987)

DOUGHERTY, S. J. *Tappi*, 72(1), 50 (1989)

GARRETT, P. R. "The mode of action of antifoams" *in Defoaming Theory and Industrial Applications*, Garrett P. R. editor, Dekker, New York, P 1-127, (1993)

HEINDEL, T. J. and MONEFELDT, J. L., *Tappi* 81(11) 149 (1998)

ISLER, W. and WIDMER, F. *Paper* 33(3) 8 (1979)

JANSE, P. C.; GOMEZ, O. and FINCH, J. A., *Can. J. Chem. Eng.*, 77, 22 (1999)

KARRAS, M. and SPRINGER, A., *Tappi*, 72(2) 155 (1989)

LINDSAY, J. D., GHIAASIAAN, S. M. and ABDEL-KHALIK, S. I., *Ind. Eng. Chem. Res.*, 34, 3342 (1995)

MAY, O. W. and BUCKMAN, S. J., *Tappi*, 58(2) 90 (1975)

PELTON, R. H., *Pulp Paper Canada*, 90(2) T61 (1989)

PELTON, R. H. and PIETTE, R., *Can. J. Ch. E.*, 70 660 (1992)

SCHULZ, E and SCOTT W "An Analysis of Air Entrainment in Secondary Fibers", Preprints, *Tappi* Papermakers Conference (1991)

WANG, G.; PELTON, R.; HRYMAK, A.; SHAWAFATY, N. and HENG, Y. M., *Langmuir* 15 2202 (1999)

CHAPTER 3

Specific Surface and Effective Volume of Water Swollen Pulp Fibers by a Permeability Method

SUMMARY:

The specific surface area per unit swollen fiber volume and the porosity of beds with a fiber concentration of 1.0 kg/m^3 were estimated from a model which employed water permeability data for the uniform pads of bleached kraft wood pulp fiber in the fiber concentration range of 108 kg/m^3 to 415 kg/m^3. The model couples a non-linear correlation between porosity and fiber concentration with the Kozeny-Carman equation. The proposed model can be applied to a wide fiber concentration range and provides estimates of the swollen fiber specific surface area and the effective specific volume.

3.1 INTRODUCTION:

In the brownstock washing process, the permeability of the pulp pad formed on the rotary drum is an important parameter in understanding the fundamentals of pad formation and washing efficiency. The pad permeability is affected by the specific fiber surface area and the properties of the effective volume of water swollen fibers. There are a number of permeability models available in the literature (Carman, 1937; Robertson and Mason, 1949; Tiller, 1975; Carlsson, 1983; Smile 1970; Wells, 1990). Among the available models, the Kozeny-Carman (Carman, 1937) equation is simple and widely

accepted. In applying this method to a pulp fiber bed, it is necessary to know the effective volume (or inversely, the porosity) and surface area of swollen fibers. Wood pulp fibers are swollen by water and are compressible, which complicates the analysis.

Robertson and Mason (1949) were the first to introduce swollen fiber properties to a modified Kozeny-Carman equation and their approach has been used extensively by many other researchers [Meyer, 1962; Gertjejansen and Hossfeld, 1967; Chan et al. 1996]. However the Robertson and Mason modified Kozeny-Carman model is strictly valid only in the low fiber concentration range (usually less than 250 kg/m^3). This limitation is a consequence of assuming a linear relationship between fiber pad porosity and fiber concentration. From a physical perspective, the Robertson and Mason model fails at high fiber concentration, because of the assumptions of constant swollen fiber surface area and constant effective volume of water swollen fiber. The surface area and effective volume of water swollen fiber pads decrease at higher fiber concentration and higher compression pressure.

Investigations of the permeability of pulp fiber mats at higher fiber concentration in the 270 – 530 kg/m^3 range and an empirical exponential permeability-moisture ratio model were reported by Carlsson (1983) and used by Kerekes and McDonald (1995) in their wet pressing model. Although Carlsson's exponential relationship between permeability and moisture ratio fits the data, the two fitting parameters do not have physical meaning and it is problematic to connect them to fiber properties.

In the modeling of brownstock pulp washer and wet pressing processes, the fiber concentration varies from a dilute fiber suspension to a relatively higher range. Neither of the two presently available models can cover the whole range. Combining the two presently available models will make the resulting mathematical model discontinuous. So there is a need to develop a new model that can solve the above-mentioned problem.

This research addresses the limitations in Robertson and Mason's model by proposing an exponential correlation between fiber pad porosity and fiber concentration and applying it to the Kozeny-Carman equation. The new model can be used in fitting the permeability data over a wider range of fiber concentrations (108 – 415 kg/m^3) and the fitting parameters are interpreted as measured characteristics of the fiber content.

3.2 THEORY

Flow through porous media can be described in the simplest case by Darcy's law:

$$Q = \frac{KA}{\mu L}\Delta P \tag{3-1}$$

where Q is the volumetric flow rate, μ is the fluid dynamic viscosity, A is the superficial pad area normal to the direction of flow, L is pad thickness, and, ΔP is the pressure drop across the pad. Darcy's law is applied to estimate the permeability of pulp pad, K.

The most widely used of the expressions relating the permeability in Darcy's law to some of the fiber properties is the Kozeny-Carman equation:

$$K = \frac{\varepsilon^3}{kS_0^2(1-\varepsilon)^2} \tag{3-2}$$

where k is an empirical constant (taken as 5.55 for pulp fiber, see [Fowler 1940]), S_0 is surface area per unit volume of solids (m^2/m^3), and ε is the porosity of the bed.

In Robertson and Mason's modification, ε and S_0 in the Kozeny-Carman equation are replaced by: the specific swollen volume (α), the specific external surface area (σ), and the fiber mass concentration in the pad (c). The modified Kozeny-Carman equations are:

$$\varepsilon = 1 - \alpha c \tag{3-3}$$

$$S_0 = \sigma / \alpha \tag{3-4}$$

$$K = \frac{(1-\alpha c)^3}{k\sigma^2 c^2} \tag{3-5}$$

According to Robertson and Mason's analysis, α in equation (3-3) lies in the range 0.003 to 0.005 m^3/(kg oven dry fiber) for most pulp fibers. When equation (3-3) is applied to a pad consistency greater than a value in the range of 200.0 kg/m^3 to 333.3 kg/m^3, the predicted porosity, from equation (3-3), will be negative resulting in a negative permeability prediction in equation (3-5).

In order to eliminate the artifact of negative porosities, and based on the available data, an exponential expression is proposed in dimensionless form:

$$\varepsilon = (1 - \theta_1)^{\gamma c} \tag{3-6}$$

where γ=1.0 m^3/kg (constant), and θ_1 is the volume fraction of swollen fiber, at a fiber concentration of 1.0 kg/m^3, which reflects the fiber water swelling property. Usually θ_1 is two or three orders of magnitude smaller than 1.0. The advantage of the form of (3-6) is that both low and high limit values of the porosity are reasonably fit. When the fiber concentration, c, approaches zero, the porosity, ε approaches 1.0. For a fiber concentration that is very large, the porosity approaches zero, but does not become negative. The parameter θ_1 is used to fit permeability data, and represents a water swollen fiber characteristic.

The parameters K, S_0, and θ_1 (from equations 3-1, 3-2 and 3-6) can be determined by non-linear regression of experimentally permeabilities, as functions of pad fiber concentration.

3.3 EXPERIMENTS ON PULP MAT COMPRESSIBILITY

The wood pulp used was an unbeaten, dry lap fully bleached softwood kraft pulp with weight average fiber length 2.01 mm and a coarseness of 0.206 mg/m. These results are based on an average of seven test runs using the Kajaani FS-200 Fiber Analyzer (courtesy of Ken Wong, Pulp and Paper Center University of British Columbia)

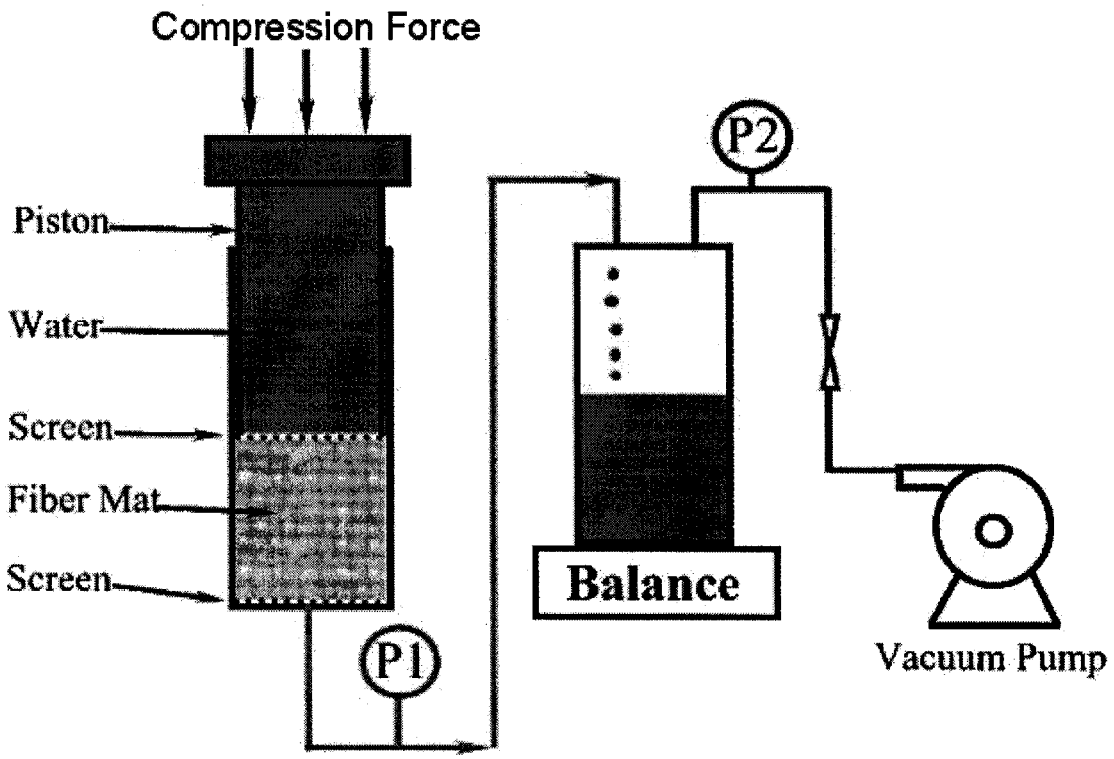

Figure 3-1 A schematic drawing of apparatus for pulp pad permeability measurements

Figure 3-1 shows a schematic diagram of our permeability apparatus. Pulp pads were formed in the permeability cell, which was a plastic column with an inner diameter of 76.2 mm and a length of 250 mm. A plastic screen on the bottom of the permeability

cell is used to filter the fibers. The screen is assumed to have a resistance $R=\Delta P/(\mu q) \approx 10^8\ m^{-1}$, where ΔP is the pressure drop (Pa) on the screen, q is the water flux (m^3/m^2s) and μ is the water viscosity (Pa.s). Vacuum and gravity were used to drive the flow through the column. DP-30 differential pressure transducers (Celesco, Toronto) were used to measure the pressure drop across the bed and the system vacuum. A vacuum control valve adjusted the pressure drop (P1) and system vacuum (P2) (see Figure 3-1) Electrical output signals from both of the pressure transducers and the electronic balance were recorded by a data acquisition system (TESTPOINT, Capital Equipment Corporation, version 2.0a 1995) at 1.0 second intervals.

In the permeation experiments the fiber bed was constrained between the plastic screen and the compression piston. The head of the compression piston was covered with a paper machine screen (with resistance of approximately $10^8\ m^{-1}$) on a porous plastic support plate. The compression piston was filled with water. The piston was raised between experiments to allow free expansion of the bed for a few minutes. This procedure was proposed by Robertson and Mason (1949) and later used by Chan et al (1996) to prevent screen blinding by fines.

A nonlinear regression program was applied to fit the permeability data (measured and calculated from equation 3-1) to the original Kozeny-Carman equation (3-2) and the proposed porosity and consistency relationship (3-6) to obtain the specific external surface area per unit volume (S_0) and specific swollen volume of the fiber bed at

fiber concentration of 1kg/m^3 (α_1). The program made use of the UNLSF subroutine in the IMSL Math Library (Microsoft Fortran 4.0 Professional) to carry out the regression analysis.

3.4 RESULTS AND DISCUSSION

Permeation experiments were conducted at a series of pad fiber concentrations, which were controlled by the position of the piston. Permeability data were calculated with equation (3-1). A direct presentation of the permeability data is shown in Figure 3-2, which gives pad permeability as a function of fiber concentration. The solid line was computed from a nonlinear regression analysis using equations (3-2) and (3-6) with a total of 33 experimental data points. The variation of permeability with this measured fiber concentration range is about three orders of magnitude, as shown in Figure 3-3. The dashed line was computed from nonlinear regression analysis of equations (3-3)-(3-5), with 12 points of low consistency data (because Robertson and Mason's model does not fit well at high consistency).

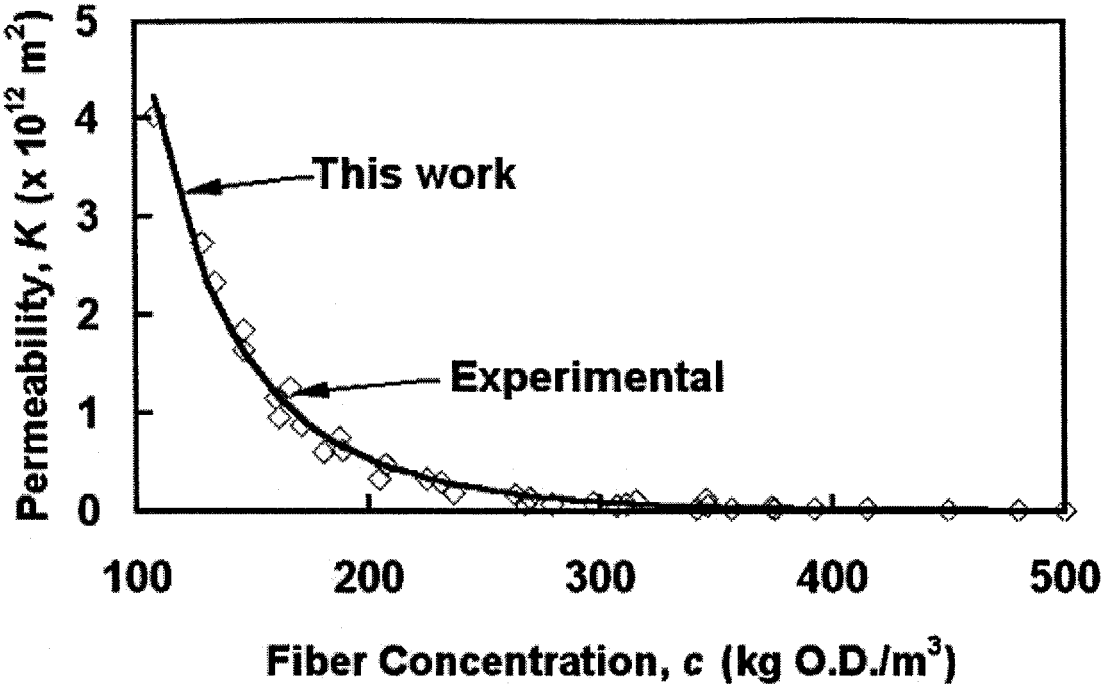

Figure 3-2 Experimental and regressed (new model) pulp pad permeability.

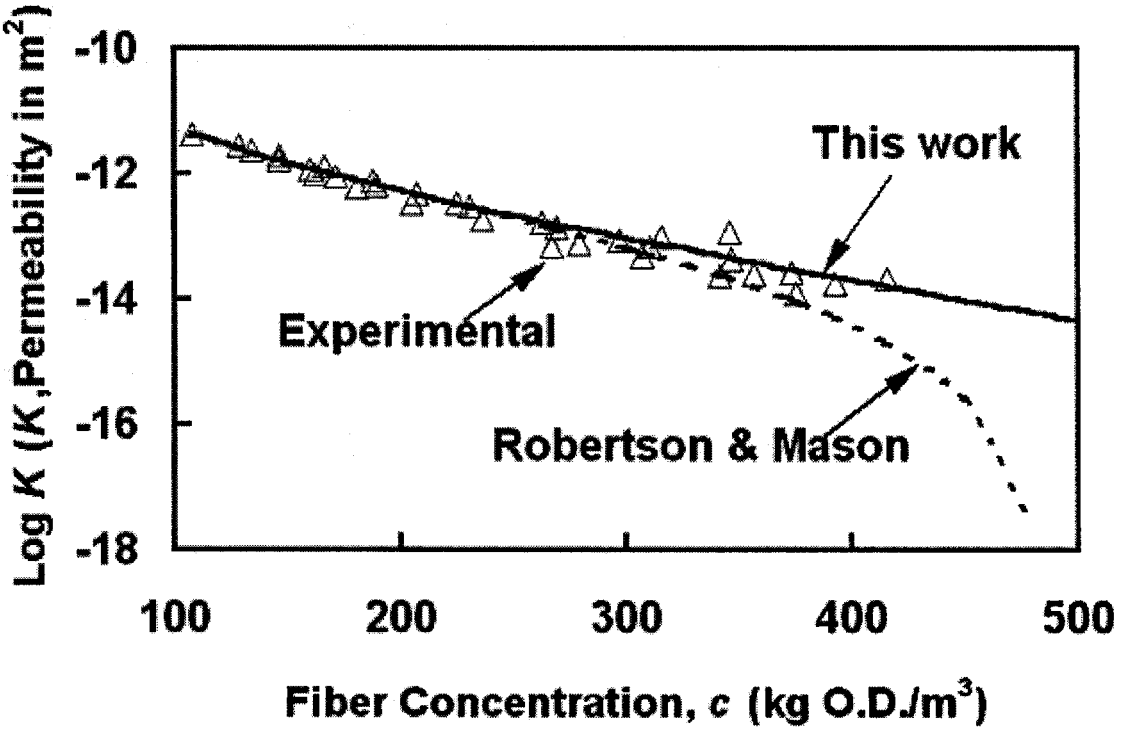

Figure 3-3 Comparison of experimental, Robertson & Mason's and the new model taking into account pulp pad permeability

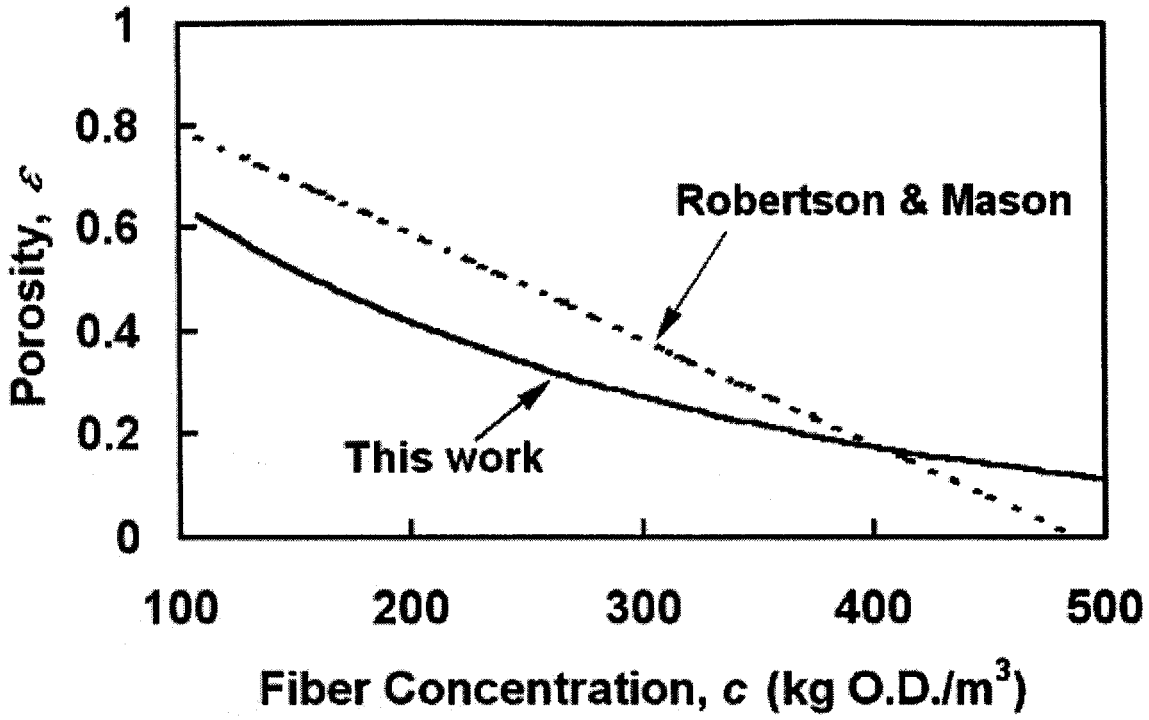

Figure 3-4 Porosity as a function of fiber concentration.

The estimated specific external surface area per unit volume of swollen fiber pad (S_0) and the swollen fiber volume fraction at a fiber concentration of 1 kg/m^3 (θ_1) was determined by nonlinear regression, using equations (3-2) and (3-6), the results were 2.71×10^5 m^2/m^3 and 4.34×10^{-3}. The specific external surface area per kilogram oven dry fiber (σ) and specific swollen volume (α) of pulp fibers in Robertson and Mason's equations (3-3)-(5) are 1.32×10^3 m^2/kg and 2.05×10^{-3} m^3/kg, respectively.

Substitution of the estimated values for θ_1 and α into equations (3-3) and (3-6) provides a relationship between the fiber consistency and porosity, as shown in Figure 3-4. It is apparent that Robertson and Mason's model gives negative porosity when the

fiber concentration is greater than 489.0 kg/m^3. This problem was successfully eliminated in the new model. Although α and σ in Robertson and Mason's model and θ_1, and S_0 in our model are regressed parameters that depend on the model form, and can be linked through their definitions.

$$\alpha = \frac{1 - (1 - \theta_1)^{rc}}{c} \tag{3-7}$$

$$\sigma = S_0 \frac{1 - (1 - \theta_1)^{rc}}{c} \tag{3-8}$$

Equation (3-7) is derived from (3-3) and (3-6), and equation (3-8) is derived from (3-4) and (3-7). The results of α and σ both from Robertson and Mason (constants dashed lines) and our new model (solid lines) are presented in Figures 3-5 and 3-6.

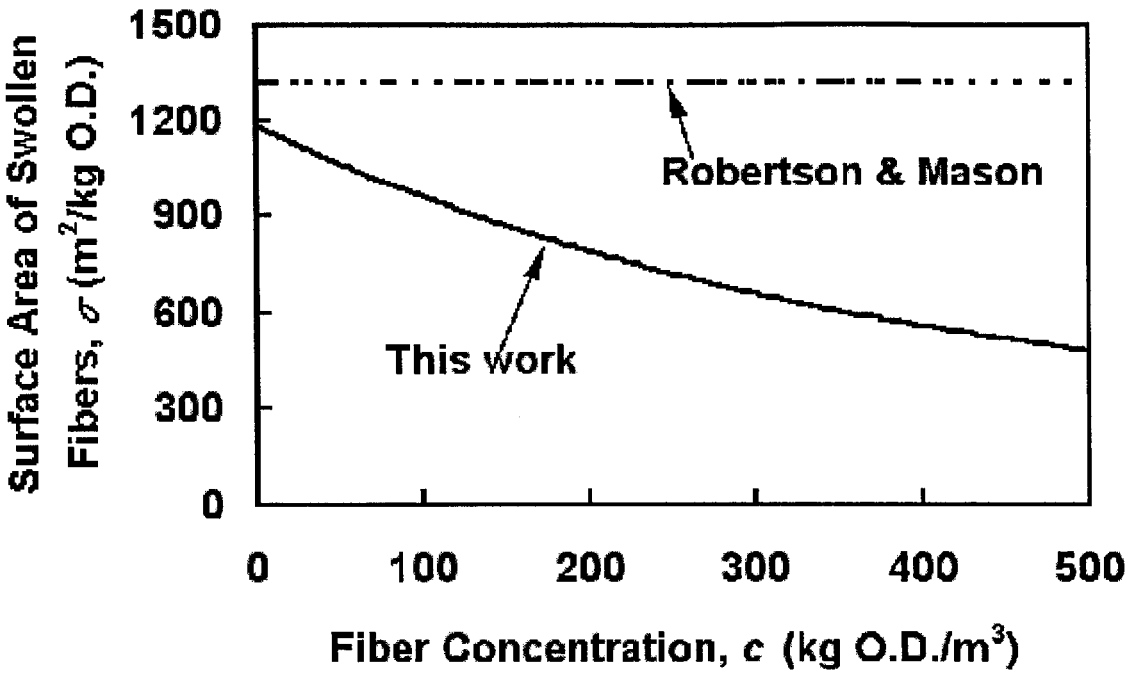

Figure 3-5 Specific Surface area of swollen fibers as a function of fiber concentration.

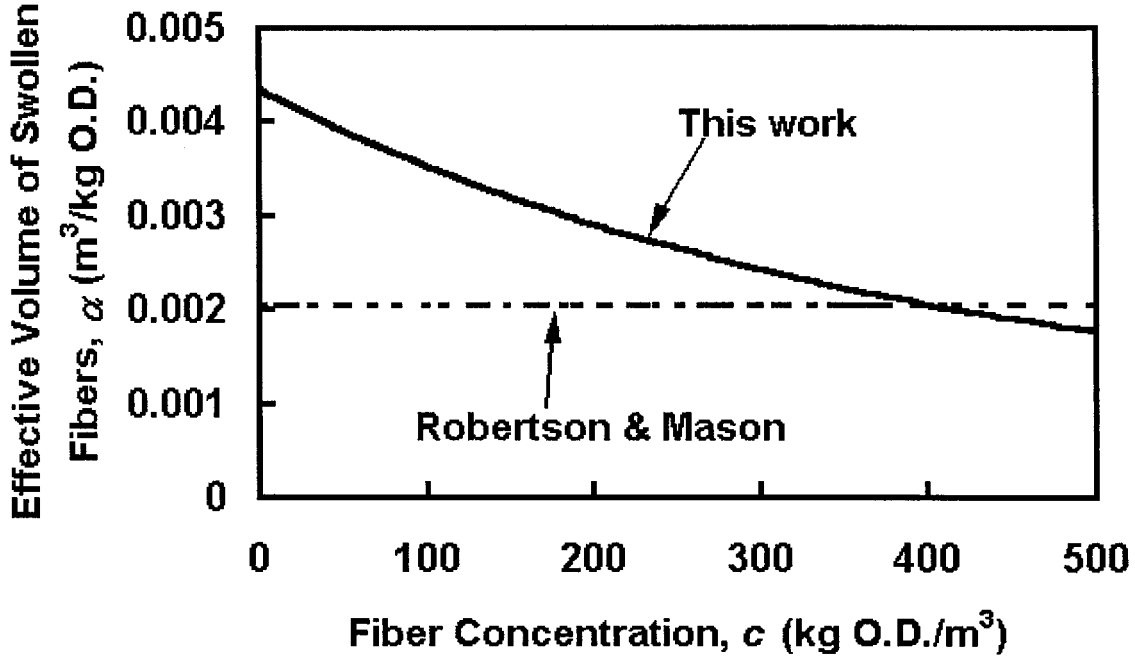

Figure 3-6 Specific effective volume of swollen fibers as a function of fiber concentration.

In Figure 3-6, α (the effective volume of swollen fiber per kilogram of oven dry fibers) from our new model is decreasing with increasing fiber consistency. This can be attributed to absorbed water, which was squeezed out from the fiber pad at high fiber concentration (corresponding to high compression pressure). In Figure 3-5, σ (surface area per kilogram of oven dry fibers) decreases with increasing fiber consistency. With increasing fiber pad concentration, the fiber-fiber contact area also increases, resulting in decreasing fiber external surface area per unit mass of fiber. We assume that the oven-dry fiber density is 1500 kg/m^3 and define the swollen fiber volume ratio as the swollen fiber volume per kg O.D. fiber divided by the volume of 1.0 kg O.D. fiber. Figure 3-7 shows the dimensionless swollen volume ratio data.

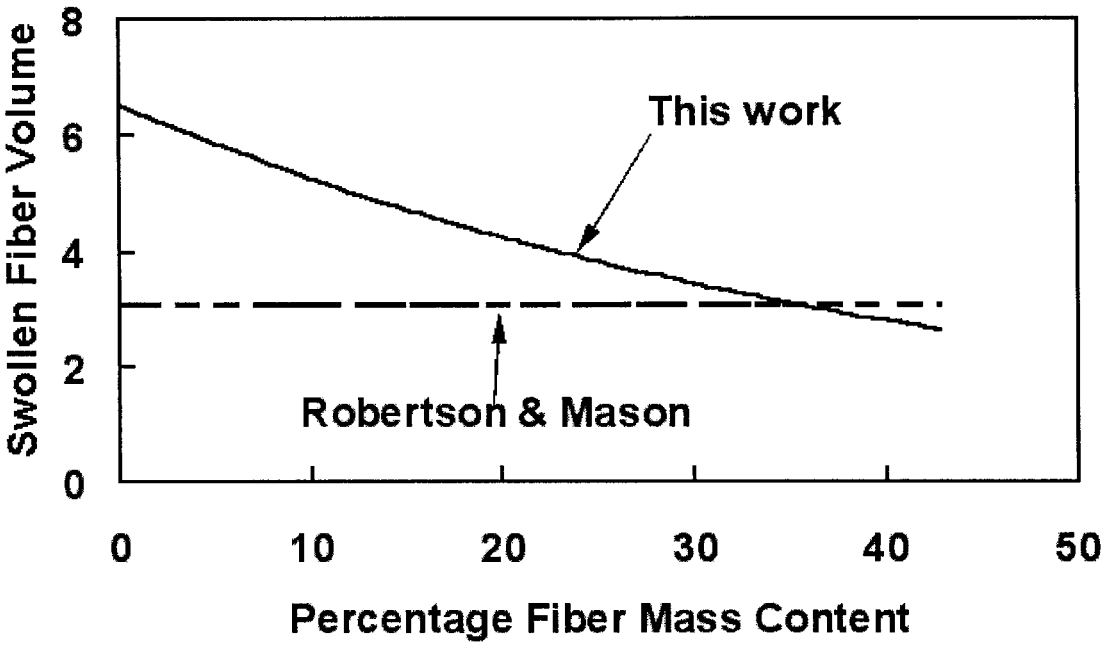

Figure 3-7 Effective volume of swollen as a function of fiber mass percentage content.

3.5 CONCLUSIONS

The following conclusions can be drawn from the results of fixed bed permeation data and the non-linear regression results:

1) Permeability data as a function of pad solids in the range of fiber concentration 108 kg/m^3 to 415kg/m^3 showed that Robertson and Mason's modified Kozeny-Carman equation is valid only in the low fiber concentration range. The assumptions of constant specific surface area and swollen fiber volume do not apply to a wide fiber concentration range.

2) With the experimentally determined permeability data, the original Kozeny-Carman equation (equation 3-2) and the proposed porosity and fiber concentration model (equation 3-6) can be applied to fit the permeability data over a large fiber concentration range. The two parameters, S_0 and θ_1 (the specific surface area per unit swollen fiber volume and the fiber pad solid volume fraction at fiber concentration of 1.0 kg/m^3) are characteristic of specific fiber types.

3) The specific surface area per kilogram of oven dry fiber (σ) and specific swollen fiber volume per kilogram of oven dry fiber (α), determined from (3-2) and (3-6), decrease with increasing fiber consistency.

REFERENCES

CARLSSON, G.; LINDSTROM, T. and FLOREN, T. *Svensk Papperstidning* r128-r134 (1983).

CARMAN, P.C. "Fluid Flow Through Granular Beds." *Trans. Inst. Chem. Engrs.* (London) 15:150-166 (1937).

CHAN, A.K.T., PELTON, R.H., ZHU, S. and BAIRD, M.H.I. "The Effects of Polystyrene Beads and Nylon Fibers on the Permeability of Compressed Wood Fiber Pads." *Can. J. Chem. Eng.* 74:229-235 (1996).

FOWLER, J. L. and HERTEL, K.L. "Flow of Gas Through Porous Media " *J. Appl. Physics,* 11:496-502 (1940).

GERTJEJANSEN, R. and HOSSFELD, R. "Gas-Liquid Relationships and their Effect upon the Permeability of Wood Pulp Pads to Water." *Tappi* 50(4):204- 208 (1967).

KEREKES, R. J. and MCDONALD, J.D. "A Decreasing Permeability Model of Wet Pressing: Application." *Tappi* 78(11):107-111 (1995).

MEYER, H. "A Filtration Theory for Compressible Fibrous Beds Formed from Dilute Suspensions." *Tappi* 45(4): 296-316 (1962).

ROBERTSON, A. A. and MASON, S.G. "Specific Surface of Cellulose Fiber by the Liquid Permeability Method.". *Pulp Paper Mag. Can.* 50:110-117 (1949).

SMILE, D. E. "A Theory of Constant Pressure Filtration." *Chem. Eng. Sci*, 25:985-996 (1970).

TILLER, F. M. "Compressible Cake Filtration". *The Scientific Basis of Filtration* edited by Ives, K. J. Noordhoff, Leyden (1975).

WELLS, S. A. "Compressible Cake Filtration Modeling and Analysis" PhD Dissertation, Cornell University (1990)

CHAPTER 4

Compressible porous and fibrous beds formed from dilute pulp suspension

SUMMARY:

A systematic experimental investigation of the formation of compressible fibrous mats formed from dilute pulp suspensions (8.00 kg/m^3 fiber concentration) has been done over a range of vacuum levels (10.0kPa – 66.7kPa). Operating vacuum and filtrate flow rate were measured by an instrumented apparatus with a computer data acquisition system. The dynamic behavior of the mat formation process, in a transparent plastic filtration cell, was observed and video taped. Dynamic fiber concentration profiles along the mat formation direction were inferred from the standard images using a grayscale analysis calibrated against a set of known concentrations. A modified filtration model for compressible fibrous mat formation was proposed based on Tiller's (1975, 1999) filtration theory. The model captures the filtrate flux and mat thickness, as a function of time and operating vacuum for a compressible mat, which has not been reported previously in the literature.

4.1 INTRODUCTION:

Brownstock washing, an important unit operation in the production of kraft pulp, is used to separate pulp fibers from pulping liquor. In this operation a large (~ 10 m long, ~4 m diameter) screened drum is partially immersed into a vat containing 1% wt wood

pulp fibers (see Figure 1-1) in aqueous pulping liquor. A vacuum is applied to the inside of the drum causing liquor to flow through the screen and subsequent build up of a fiber pad on the drum surface. The drum rotates at about 4 RPM causing an approximately 40 mm thick fiber pad on the drum screen surface to emerge from the vat. Water is sprayed onto the fiber pad after withdrawal from the vat to displace the liquor from the fiber pad. The pad is scraped from the drum surface just before the screen re-enters the vat.

In previous work, we have extensively investigated the displacement washing zone. We have shown that the introduction of cationic polymers into the wash water gives improved displacement washing by the selective formation of lignin-polymer precipitates in the most open channels of the pad (Lappan et al, 1996). For an overview of this work see Pelton (1999).

Our current activities are focused on the pad formation process, which occurs in the vat. Recently we have shown that the presence of dispersed air causes channels to form in the pad, which lowers the liquor flux by as much as a factor of ten compared with air-free pulp (Wang et al, 2001). Most of the negative effects due to the presence of dispersed air can be eliminated by defoamer addition. Defoamer does not remove air from the pulp, instead it appears to destabilize the bubbles allowing them to pass through the pad and thus not interfere with liquor flow and thus production.

One of the objectives of our current work is to develop mechanistic models for the pulp pad formation process, which is essentially a filtration. In the case of wood pulp, the analysis of filtration is complicated by the fact that the fibers are not uniformly dispersed,

but are present as flocs (Kerekes, 1983). A further complication is that pulp pads are compressible causing the volume fraction of solids in the pad to vary in the flow direction and to be a function of the applied pressure.

Empirical models of brownstock drum washers have been developed (Han, 1989; Wang, 1993; Kempe, 1995). Experimental grayscale analysis of a still pulp suspension was reported by Kerekes and Schnell (1995), but the present work is the first experimental characterization of dynamic compressible pad formation similar to that in a brownstock drum washer.

One of the first filtration models is Ruth's (1933) cake filtration model. Meyer (1962) proposed a differential equation for pulp fiber filtration process, but only a very simplified tentative solution was provided. Other cake filtration models include those of Smile (1970), Atsumi and Akiyama (1975), Wakeman (1978) and Stamatakis and Tien (1990, 1991). Each offers improvements in numerical methodology with respect to the moving interface, but are restricted in their application to compressible pulp fiber systems. Jonsson and Jonsson (1992a, 1992b) propose a dynamic model for filtration and wet pressing of a compressible porous media with a fixed mass of fiber and fixed relative thickness (Δy) in each isotropic layer.

The model due to Tiller et al. is the most commonly accepted in filtration theory, because of its reliability and relatively wide range of applications. Tiller's model is very successful in traditional cake filtration, but the parameters pertinent to wood fibers are not available. Empirical filtration formulae developed for other materials are doubtful when applied to a wood pulp fiber mat, because of the characteristics of water swollen,

compressible wood fibers. Some empirical relationships between volume reduction and applied pressure are available in the literature (Qviller 1938; Campbell, 1947; Ingmanson, 1952, 1954). These correlations are limited to a narrow pressure range, and no general wood pulp fiber bed compressibility correlation is available in the literature.

This work proposes constitutive equations for compressibility and permeability by considering three pulp fiber characteristics (water swell, compressibility, and specific surface area) to be used with Tiller's model in a comparison with experimental measurements of pulp fiber-water filtration processes.

4.2 EXPERIMENTAL:

1) Apparatus

Figure 2-1 shows a schematic diagram of the experimental apparatus, which is same as that in Chapter 2. A metal washer screen with a measured resistance of $R=\Delta P/(\mu q) \approx 1.0\times10^{8}\ m^{-1}$ formed the top of the filtration cell. The resistance of the pipe connecting the filtration cell and vacuum accumulator was determined to be $R=\Delta P/(\mu q) \approx 1.2\times10^{9}\ m^{-1}$.

1.1) Data acquisition system

The operating vacuum was measured by pressure sensor (Celesco DP30-0001-111) via a DAS-802 A/D board (Keithley Metrabyte Co.) to a PC. A digital balance (Mettler PM16) was used to measure the collected mass of filtrate (water), which was directly connected to the PC. TESTPOINT (Capital Equipment Corporation, version 2.0a

1995) software was employed to collect data for vacuum and mass of filtrate, at a frequency of 1.0Hz.

1.2) Pulp slurry re-circulation and Vacuum System

A Moyno progressing cavity pump (A1B SS03 AAA) was used to pump the pulp slurry from the pulp slurry tank into the vat. It overflowed through the other end of the vat and flowed back to the pulp slurry tank. A Welch duo-seal vacuum pump (Sargent-Welch Scientific Co. model: 1400) was used to generate the vacuum. An air accumulator was employed to stabilize the vacuum. Vacuum was applied to the top of the filtration cell through a tube and control valve. With applied vacuum the pulp slurry moved toward the screen and the mat began to grow. The applied vacuum was adjusted manually to the desired vacuum level by a vacuum adjustment valve, which was on top of the air accumulator. In this experiment, vacuum levels of 10.0kPa, 20.0kPa, 40.0kPa, 66.7kPa (or 75, 150, 300, 500 mmHg), were set.

1.3) Optical system

A light table (Visual Plus, Model VP-4050v with viewing size: 310mm×216mm) was used as the background light of the filtration cell because of its homogenous lighting effect, which was important for image analysis. A digital camcorder (Canon (1998) ZR with 30 frames per second and 720×480 pixels per frame) was employed for taking videos of the visualized filtration cell.

2) Materials and Procedure

The wood pulp fibers used were fully bleached Northern Canadian unbeaten softwood kraft pulp. The mean fiber length of the pulp was measured to be 2.01 mm with a coarseness of 0.206 mg/m. These results were based on an average of seven test runs on a Kajaani FS-200 Fiber Analyzer (courtesy of Ken Wong, Pulp and Paper Center, University of British Columbia) .

In a typical experiment, the pulp slurry in vat and tank consisted of 40.0 liters of water and 434.1 gram of air dried pulp fiber (about 7% wt water content) mixed to a pulp slurry. After activating the slurry pump, the mixer in the tank, and the mixer in the vat, the pulp slurry circulated for about 10 minutes. The vacuum pump was started and the vacuum level set to the desired value by manually adjusting the valve on the top of vacuum accumulator. Water was added to the top of filtration cell, which was located between the filtration screen and connecting pipe (from filtration cell to filtrate tank). The purpose of this operation was to eliminate the dead time in the filtrate flux measurement. The valve was slowly opened on the top of the filtration cell and the pulp slurry was allowed to touch the filtration screen, then the valve was closed. The background lighting and digital camcorder was set up for image capture, with the white balance and exposure level set manually (Canon, 1998). Filtration measurements started when the control valve on the top of filtration cell was opened in a quick motion. In order to test repeatability, 3 runs were taken at each vacuum level for a total of 12 runs, the repeatability is pretty good. After each experiment, the pulp slurry pump and mixers were kept running and the fiber slurry in the vat sampled (total mass measured was 1050.33 g). The oven dry fiber mass in this sample measured

8.38 gram, oven dry fiber density is 1500 kg/m^3, so the fiber (oven dry) concentration was 8.00 kg/m^3 (or 0.798% mass consistency).

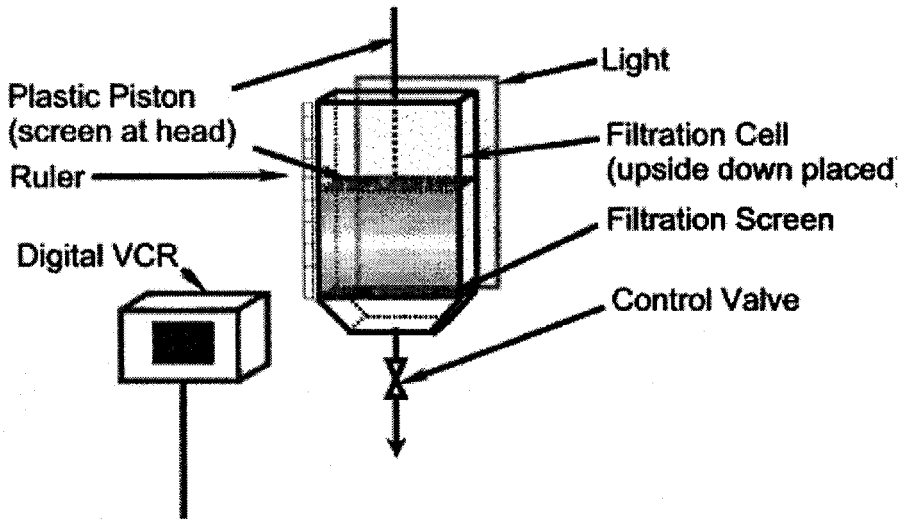

Figure 4-1 Calibration experiment of grayscale level vs. fiber concentration

3) Calibration of grayscale level and fiber concentration

A dilute pulp slurry of 0.1 % mass concentration was introduced in a small tank with about 10 gram of air-dried pulp (about 7% water content). The filtration cell was placed upside down (see Figure 4-1), with the camcorder and background light the same as that used in mat formation process studies. The water was allowed to drain out very slowly to achieve a relatively homogenous mat. At higher fiber concentrations, we manually compressed the fiber mat. Images were taken at mat thickness from 150 mm to 10 mm at a 10 mm intervals. The cross section area of the filtration cell was 0.155×0.02

m^2. From each calibration image we found the mat thickness by checking the ruler at the left side of the image, so with the mat thickness and cross section area of the filtration cell, the volume of mat for each image was determined. The oven dry fiber weight was measured after finishing the calibration image taking process. The fiber concentration for each image was total oven dry mass of fiber divided by total mat volume. The average grayscale level of the mat image was determined by a simple Fortran code with a Postscript image file as the input grayscale data file. A total of 85 image files corresponding to 85 experimental data points, with grayscale levels corresponding to fiber concentrations from 10.77 to 198.92 kg/m^3, were regressed using fourth order polynomials. The regressed result and original experimental data points are plotted in Figure 4-2. The grayscale levels were near constant at high fiber concentration (over 160 kg/m^3). That means the error of fiber concentration was much larger than that in low fiber concentration area. Our research focused on mat formation from dilute fiber suspension rather than fiber mat compression, with specific interest in the low fiber concentration area. So the inferred fiber concentration in this higher fiber concentration area either were deleted (if it was not reasonable) or used only as a reference.

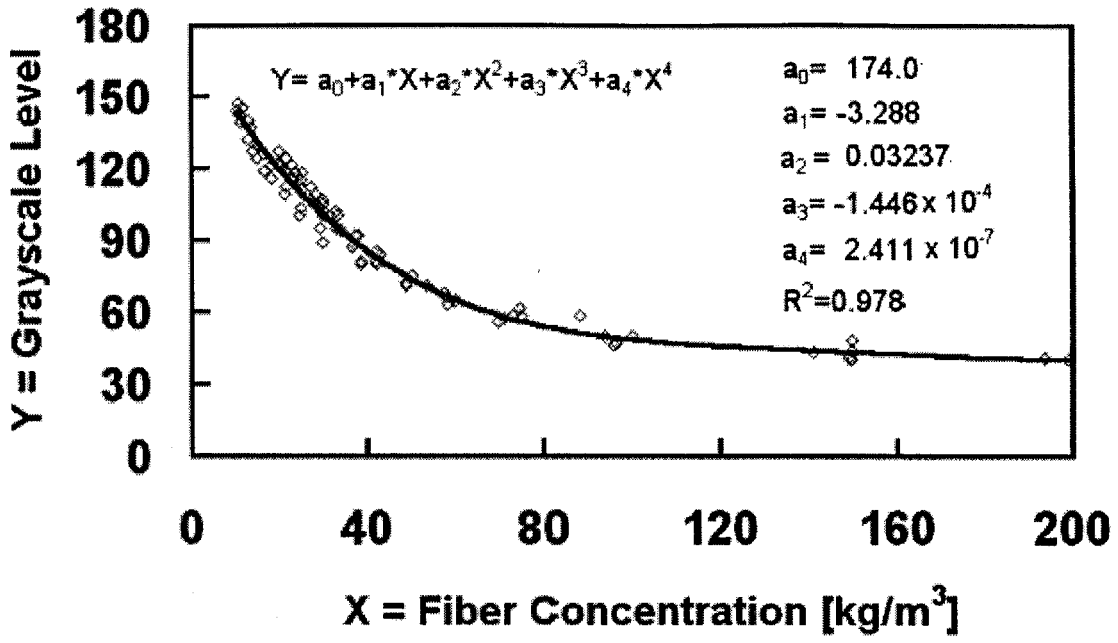

Figure 4-2 Correlation between fiber concentration and grayscale level

4.3 EXPERIMENTAL RESULTS:

Single frame images were taken from the digital video using Adobe Premiere 5.0 (Adobe Systems Inc.) at 5, 10, 15, 20, 25, 30, 60, 120 seconds for each run. The image files were saved as Postscript files. Data in the image files were converted to dynamic grayscale distribution plots, and with the correlation on Figure 4-2, were converted to local mat fiber concentration plots. Estimated local fiber concentrations greater than 150 kg/m^3 were not very accurate, because the grayscale levels were nearly constant at high fiber concentration (see Figure 4-2).

Figure 4-3. Sample video frame at vacuum level of 20kPa and time of 60 seconds

Figure 4-3 is a sample image of the mat formation process at an operating vacuum of 20kPa after 60 seconds from the beginning of filtration process. The left side of the image is a ruler. This image was cropped from top of the filtration cell (0.00 m to 0.13m) to keep the fiber mat in the image (without ruler) and saved as a Postscript file (350 × 437 pixels, Height×Width). The average grayscale number of each line of pixels (total 437) in the image was calculated. Along the mat formation direction of 0.130 m, there were a total of 350 pixels, so each pixel corresponds to 3.714×10^{-4} m. The average grayscale level along the mat formation direction is shown in Figure 4-4, the grayscale vs distance line was composed by hundreds of data points, which corresponds to the pixels of the image on Figure 4-3.

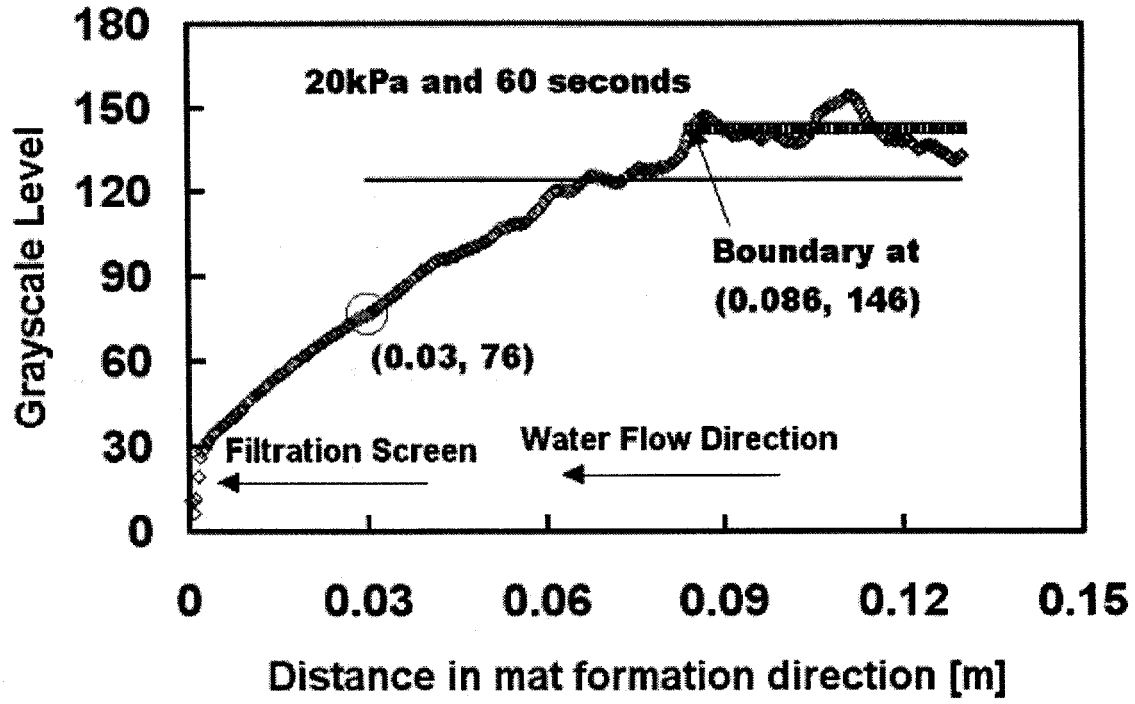

Figure 4-4. **Average grayscale level of horizontal lines of pixels *vs.* distance in mat formation direction for Figure 4-3**

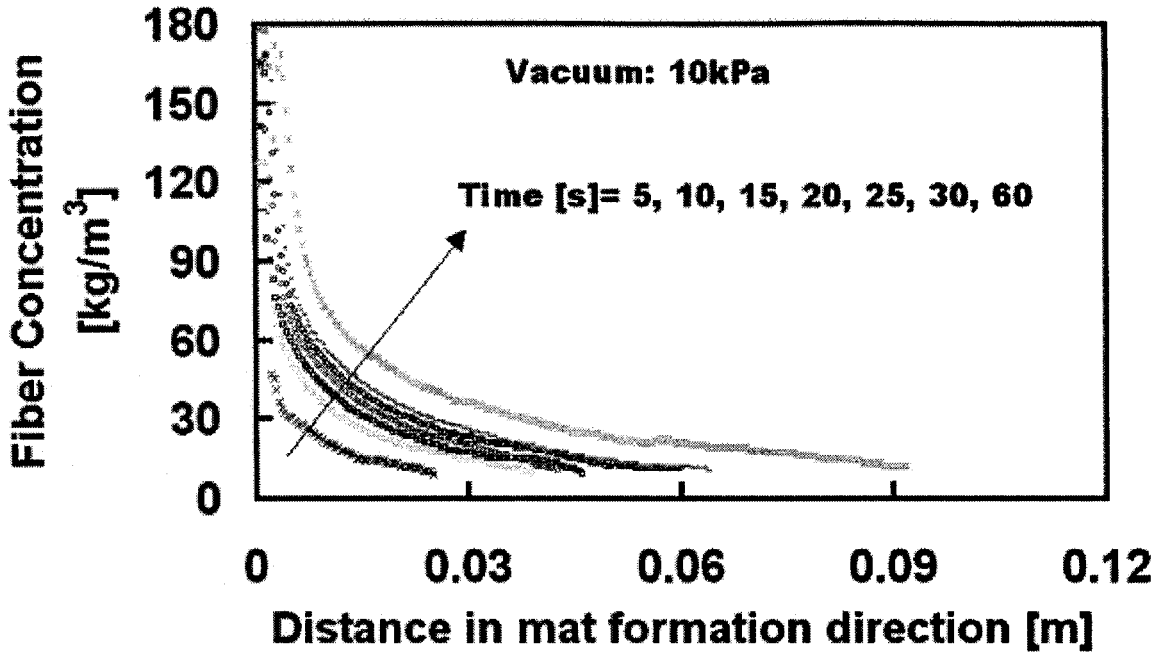

Figure 4-5. Fiber concentration profiles at vacuum level of 10.0 kPa

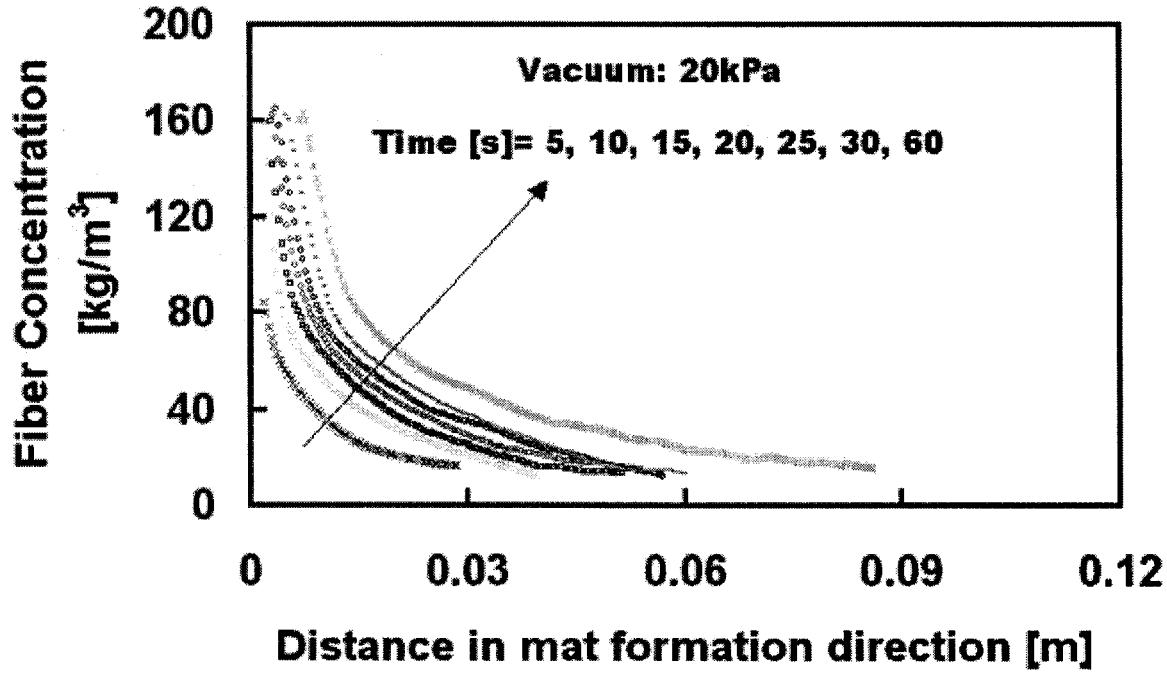

Figure 4-6. Fiber concentration profiles at vacuum level of 20.0 kPa

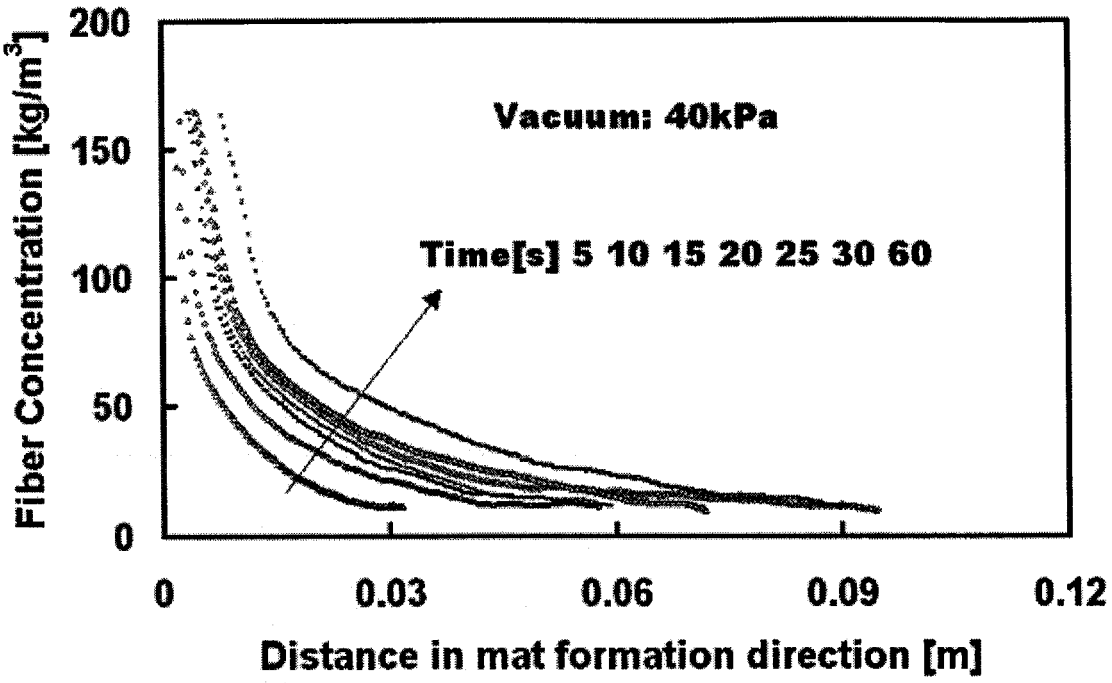

Figure 4-7. Fiber concentration profiles at vacuum level of 40.0kPa

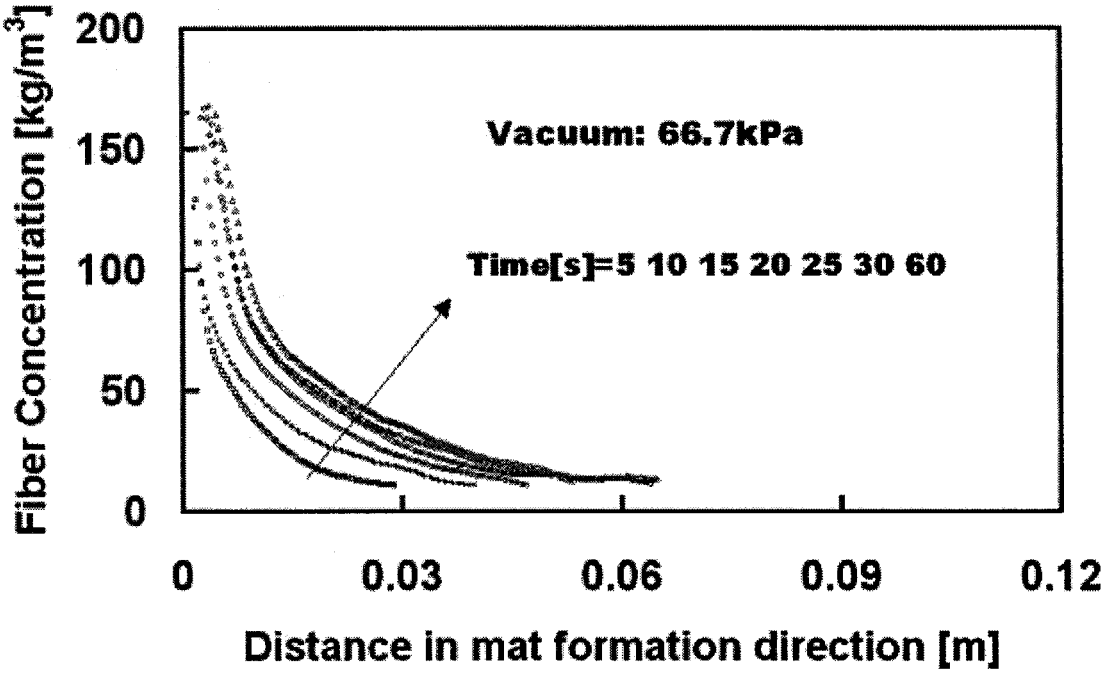

Figure 4-8. Fiber concentration profiles at vacuum level of 66.7 kPa

The mat thickness was defined (Definition 1) as the distance from the top of the filtration cell to the point, x, where the grayscale level reached the average grayscale level of the remaining part of filtration cell (from x m to 0.130 m). For example, in Figure 4-4 at x = 0.086 the average grayscale of the rest of cell (from x = 86 mm to 13 mm) is 146, so this is taken as the boundary between mat and fiber suspension. The suspension area has a constant concentration with little variation due to its heterogeneity. The focus of this study was the fiber mat and its dynamic formation process, so only the mat portion of the image analysis is shown in Figures (4-5)-(4-8). Mat-suspension boundaries were located using the fiber concentration plots. The mat thickness for experiments at operating vacuum levels of 10 kPa, 20 kPa, 40 kPa and 66.7 kPa are shown in Figure 4-9.

In order to test the above definition of mat thickness, an alternate mat boundary definition was used, based on a threshold grayscale number. The mat thickness was defined (Definition 2) as the distance x in the image with an average grayscale level less than that of fiber suspension solution (8.0 kg/m^3 O.D. fiber, in this case grayscale level is 150, see Figure 4-2). Comparing Figures 4-9 and 4-10, the mat thickness defined by definition 2 is greater than that defined by definition 1, there is more scatter in the data, though the trend of the estimated mat thickness is similar. One explanation for the difference in mat thickness estimates is that the threshold value used in Definition 2 (boundary at grayscale level of 150) includes pulp suspension not consolidated into the mat structure. Thus, the estimated mat thickness defined by the second method overestimates the mat thickness. An absolute threshold grayscale may provide a method

for mat thickness estimates, but the threshold grayscale value must come from experience or other evidence.

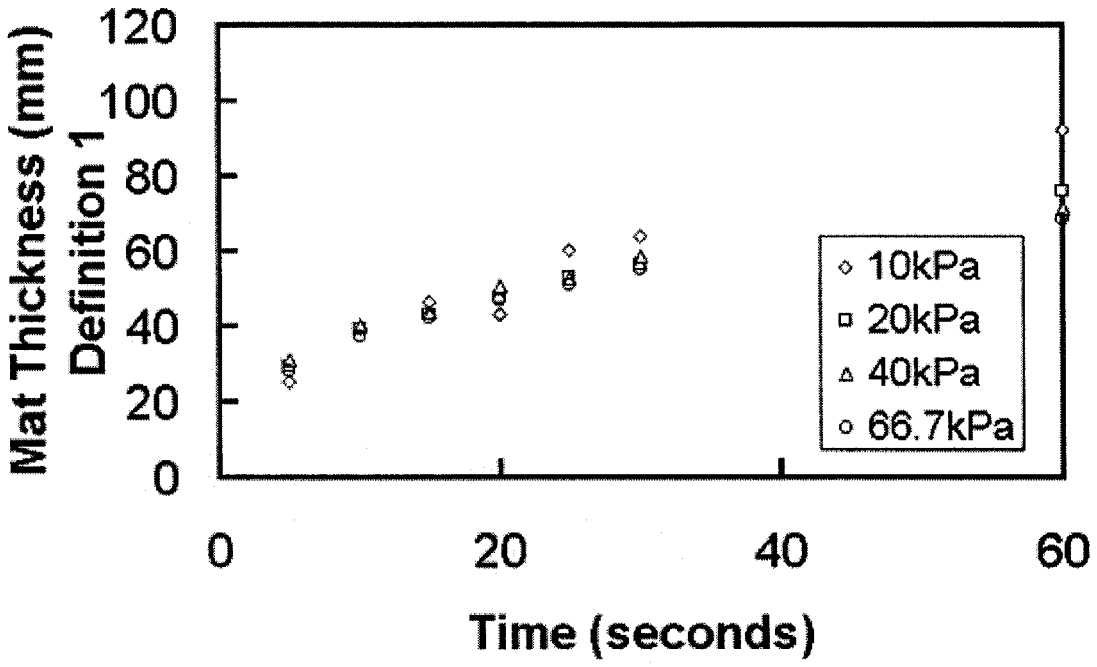

Figure 4-9. Mat thickness at varied vacuum levels with definition 1

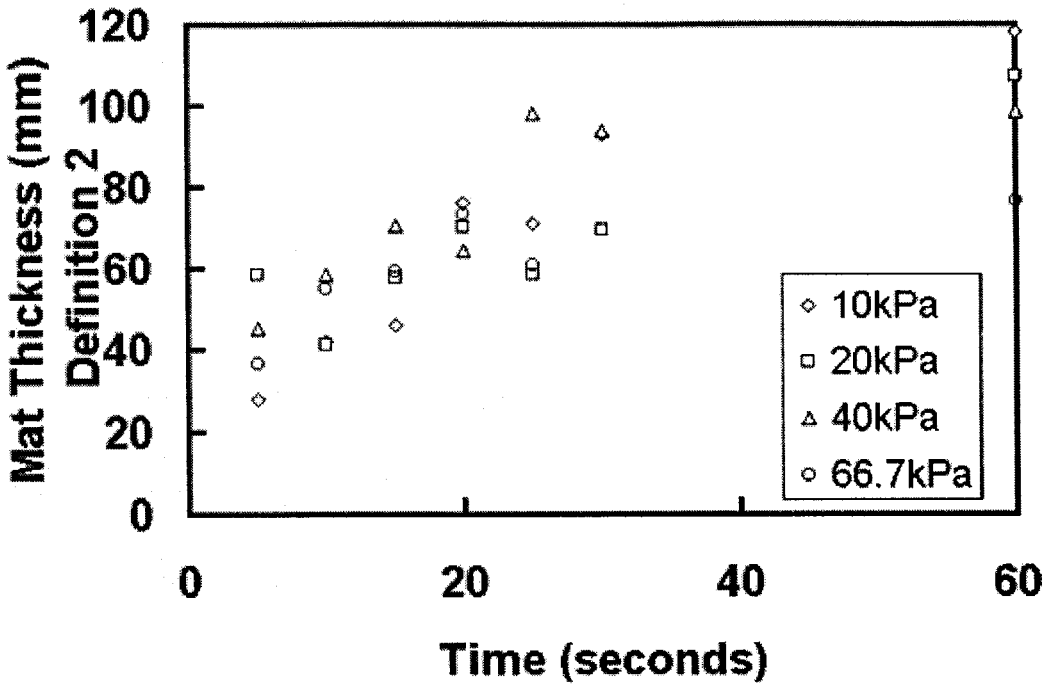

Figure 4-10. Mat thickness at varied vacuum levels comparing with definition 2

In both Figures 4-9 and 4-10, the operating vacuum had little influence on the mat thickness growth, but it strongly influenced the mat concentration profile at low vacuum range (10 kPa – 20 kPa). Figure 4-11 is a plot of the fiber concentration profile after 10 seconds; similar results were also found in plots of 5, 15, 20, 25 seconds. The influence of operating vacuum levels greater than 20 kPa on the fiber concentration profile diminished (the fiber concentration profile at a vacuum of 66.7 kPa was within experimental error of the 40 kPa data).

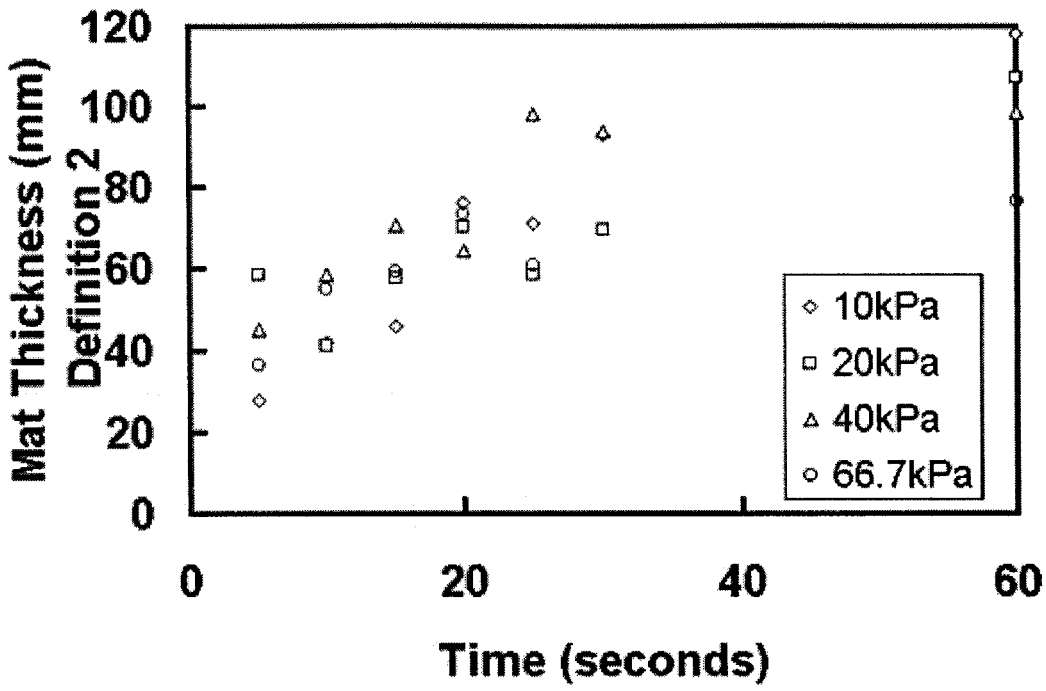

Figure 4-11. Fiber concentration profile at different operating vacuum (at 10 seconds)

The total volume of the filtrate was measured as a function of time and the results are shown in Figure 4-12. The filtrate flux trend (Figure 4-13) appears similar to other conventional filtration experiments. From our observations, the compressible porous and fibrous mat was composed of relatively uniform layers. No flow channels in the fiber mat were found in this fiber-water system, through observations with dye tracer injection into the pulp/water suspension. Similar results have been reported previously (Wang, et al, 2002).

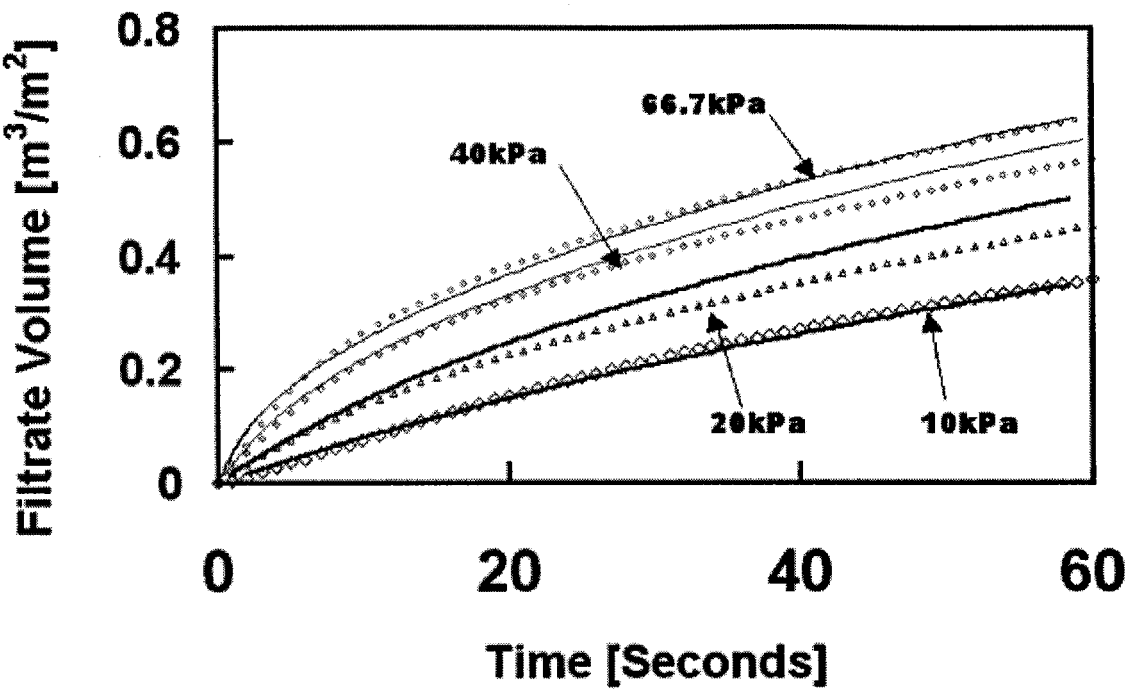

Figure 4-12. Experimental and calculated filtrate volume as a function of vacuum level.

Tiller's model requires permeability and compressibility correlations for pulp fiber. Compressibility data were measured and a simple correlation fitted, as shown in Equation (4-1) and Figure 4-14.

$$C = ap^4 + bp^3 + cp^2 + dp + e \tag{4-1}$$

$$a = -3.517 \times 10^{-18}$$
$$b = 1.160 \times 10^{-12}$$
$$c = 1.426 \times 10^{-7}$$
$$d = 8.903 \times 10^{-3}$$
$$e = 71.91$$

where, p [Pa] is applied pressure and C [kg/m^3] is the fiber concentration.

The most widely used of the expressions relating the permeability in Darcy's law to some of the fiber properties is the Kozeny-Carman equation:

$$K = \frac{\varepsilon^3}{kS_0^2(1-\varepsilon)^2} \tag{4-2}$$

where k is an empirical constant taken as 5.55 for pulp fiber (Fowler, 1940), S_0 is surface area per unit volume of solids (m^2/m^3), and ε is the porosity of the bed. An empirical expression for ε was proposed in dimensionless form:

$$\varepsilon = (1-\theta_1)^{\gamma C} \tag{4-3}$$

where γ=1.0 m^3/kg (constant), and θ_1 is the solid fraction of swollen fiber bed at a fiber concentration of 1.0 kg/m^3. The parameter θ_1 was used to fit permeability data, and represents a water swollen fiber characteristic. The estimated value of S_0 is 2.71×10^5 m^2/m^3 and θ_1 is 4.34×10^{-3}

4.4 TILLER'S FILTRATION MODEL AND MODELING RESULTS

Tiller's cake filtration model is composed of a mass balance, force balance, Darcy-Shirato Equation, empirical constitutive compressibility model and empirical constitutive permeability model. From an over-all system view, the mass balance can be written on a unit area basis in the form:

Mass of slurry = mass of cake + mass of filtrate:

$$w/s = w/s_c + \rho\, v \tag{4-4}$$

where w is the mass of dry solids per unit area, v the filtrate volume per unit area, s the mass fraction of solids in slurry, s_c the average mass fraction of solids in the cake, and ρ the density of the filtrate. Solving for v in equation (4-4) yields:

$$v = \frac{1 - s/s_c}{\rho s} w \tag{4-5}$$

From the definition of s_c,

$$s_c = \frac{\rho_s(1-\varepsilon_{av})}{\rho_s(1-\varepsilon_{av}) + \rho\varepsilon_{av}} \tag{4-6}$$

where the average porosity of the cake is

$$\varepsilon_{av} = 1 - \frac{\int_0^p dp_s / \alpha}{\int_0^p \frac{dp_s}{\alpha(1-\varepsilon)}} \tag{4-7}$$

and α is the specific resistance ,

$$\alpha = \frac{1}{\rho_s(1-\varepsilon)k} \tag{4-8}$$

Tiller's key filtration equation is:

$$vq_1 = \frac{\sigma - s(\sigma-1)}{\mu\rho_s s} \int_0^{p-p_1} \frac{dp_s}{\alpha} - \frac{1}{\mu\rho_s} \int_0^{p-p_1} \frac{dp_s}{\alpha(1-\varepsilon)} \tag{4-9}$$

where σ ($=\rho_s/\rho$), is the specific gravity of the dry solids. The pressure p_s is the mechanical pressure on the solids, and p_l is the pressure drop on the filtration screen. Tiller's original empirical compressibility and permeability models for cake particle filtration were of the form:

$$\varepsilon_s = \varepsilon_s^0 \left(1 + \frac{P_s}{P_a}\right)^{\beta} \tag{4-10}$$

$$k = k_0 \left(1 + \frac{P_s}{P_a}\right)^{-\delta} \tag{4-11}$$

Where ε_s is cake solidosity (solid volume fraction) and k is the permeability. are empirical β , δ , ε_s^0 , k_0 constants for materials. Values of these constants in the two constitutive equations for various types of cakes can be found in the literature. Pulp fiber characteristics were not considered by the above two constitutive equations.

A number of sample calculations at various vacuum levels were done with Tiller's filtration equations and the fiber constitutive equations (4-1)-(4-3). The filtrate volume and flux are shown in Figures 4-12 and Figure 4-13.

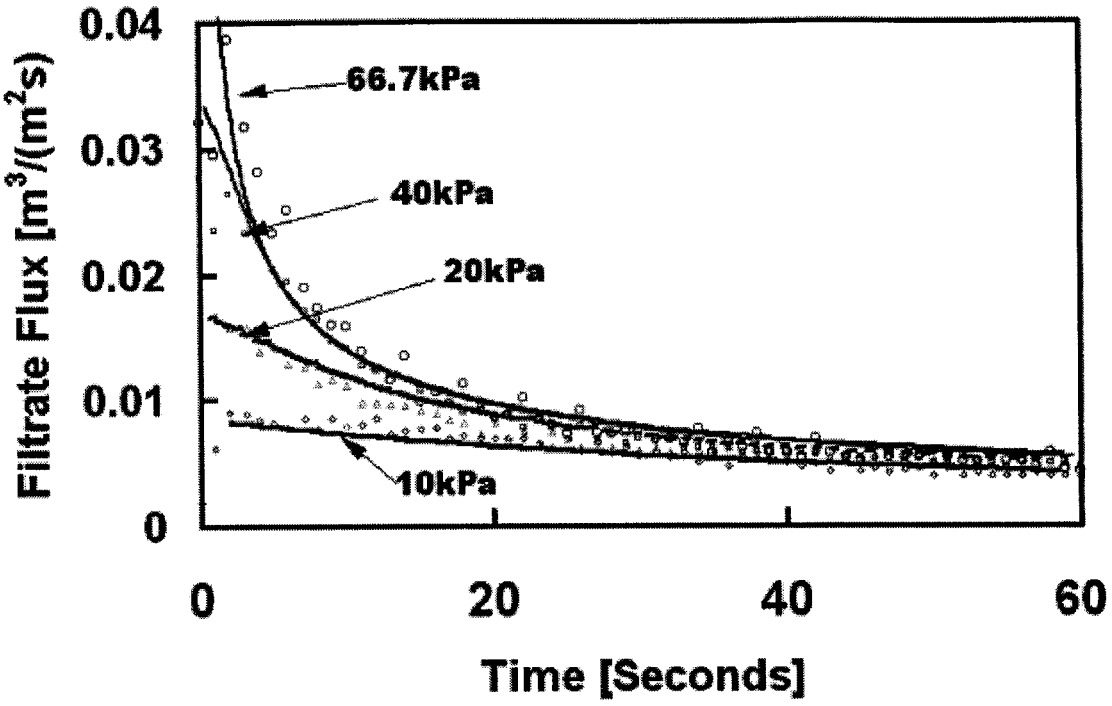

Figure 4-13. Experimental and calculated filtrate flux as a function of vacuum level

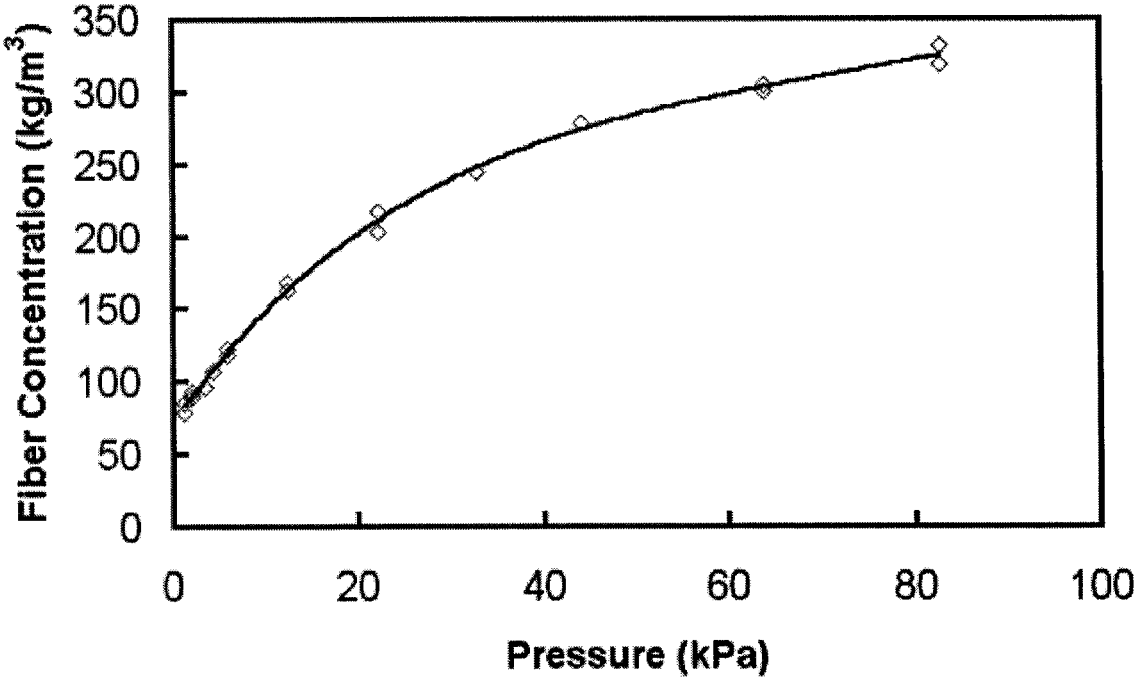

Figure 4-14. Fiber compressibility experimental measurements

From the system total mass balance

$$L + V = L^*C_{avg}/C_0 \qquad (4\text{-}12)$$

where L is the fiber mat thickness and V is the filtrate volume, C_{avg} is the average fiber concentration in the mat and C_0 is the fiber concentration in the slurry (8.0 kg/m^3 in this case). Although C_{avg} varies with the pressure drop through a mat, in a constant pressure filtration process, C_{avg} may reach a steady state constant value in seconds. It is usually assumed to be constant and equal to the experimental value obtained at the end of a run [2]. In this case, C_{60} , the average mat fiber concentration at 60 seconds, was taken to be C_{avg} for the cake thickness calculation. The experimentally measured values of C_{60} at various vacuum levels are shown in Figure 4-15 and the estimated mat thickness is shown in Figure 4-16

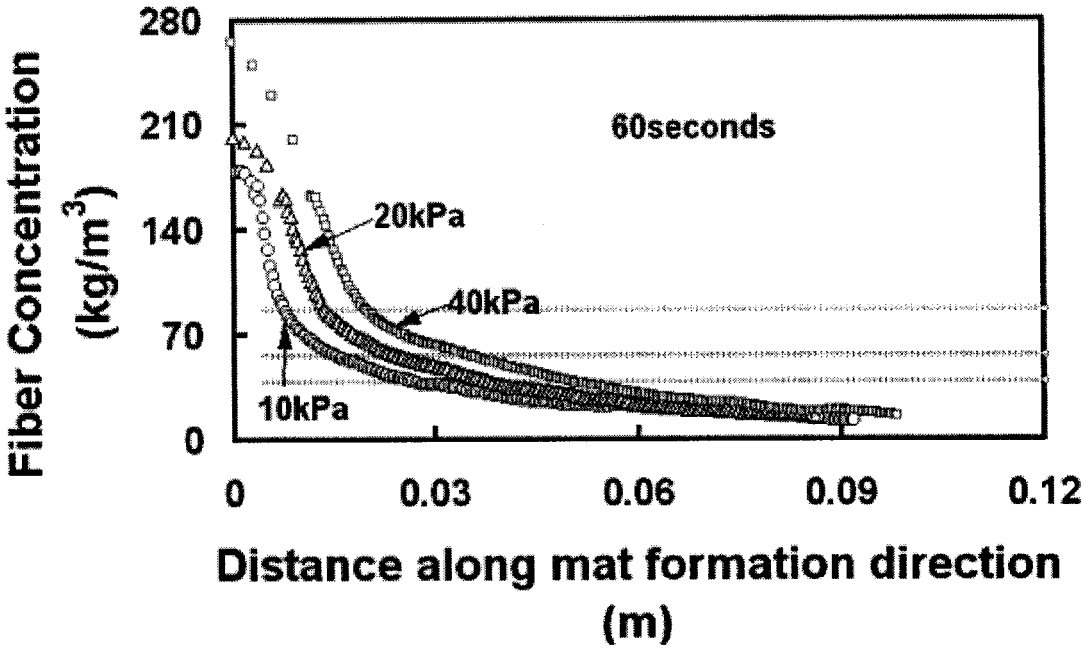

Figure 4-15. Experimental average fiber concentration in the mat after 60 seconds at varied vacuum levels

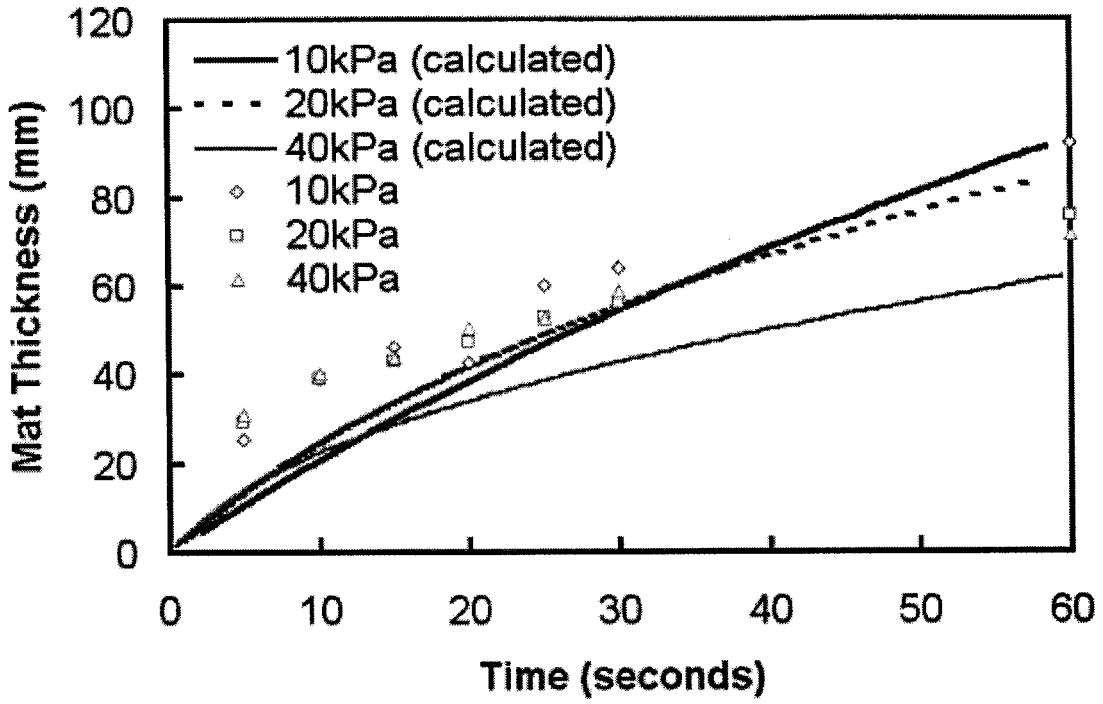

Figure 4-16. Experimental and calculated mat thickness as a function of vacuum level

The flux calculation due to Tiller's model agrees with the experimental data very well at each tested vacuum level. Mat thickness can only be estimated with calculated filtrate volume (V) and average fiber concentration in the mat (C_{avg}) in equation (4-12). The assumption that C_{avg} is approximated by C_{60} increases the error of the mat thickness calculation during the initial few seconds of filtration (see Figure 4-16), but the calculated mat thickness agrees with the experimental data considering the error in the fiber mat thickness measurements. As seen in Figure 4-16, the vacuum level has very little influence on the mat thickness.

4.5 CONCLUSIONS:

The dynamic fiber concentration profiles of compressible porous fibrous beds formed from dilute pulp slurry were measured with grayscale analysis. A clear boundary between the fibrous mat and slurry did not exist. The fibrous mat was composed of layers of compressed fibers. Increasing operating vacuum did not increase the thickness of the fiber mat, but did increase the fiber concentration in the mat with diminishing changes at vacuum levels above 20 kPa. The filtrate flux increased with increasing vacuum levels for short times (less than 20 seconds). The concentration profiles, boundary estimate and filtrate flux provided an experimental basis to validate a model.

Tiller's cake filtration model was modified with experimental fiber compressibility and permeability correlations. The calculated filtrate flux at varied vacuum agreed with experimental measurements very well. The dynamic mat thickness can also be estimated with the calculated filtrate volume and the observed fiber concentration in the mat.

REFERENCES

ATSUMI, K; AKIYAMA, T. "A Study of Cake Filtration" *J. of Chemical Engineering of Japan*, 8, 6. (1975)

CAMPBELL, W. B. "The Physics of Water Removal". *Pulp Paper Mag. Can.*, 48,3. (1947)

CANON ZR digital video camcorder, *Instruction Manual*, Canon Inc. (1998).

CARMAN, P. C., "Fluid Flow Through Granular Beds", Trans. Inst. Chem. Engrs. (London) 15:150-166 (1937)

FOWLER, J. L.; HERTEL, K. L. "Flow of Gas Through Porous Media." *J. Appl. Physics.*, 11, 496. (1940)

INGMANSON, W. L. "An Investigation of the Mechanism of Water Removal from Pulp Slurries." *Tappi*, 35(10), 439. (1952)

INGMANSON, W. L.; WHITNEY, P. P. "The Filtration Resistance of Pulp Slurries." *Tappi*, 37(11), 523. (1954)

JONSSON, K. A.; JONSSON, B. T. L. "Fluid Flow in Compressible Porous Media: I: Steady-State Conditions." *AIChE J.*, 38(9), 1340. (1992)

JONSSON, K. A.; JONSSON, B. T. L. "Fluid Flow in Compressible Porous Media dynamic behavior" *AIChE J.*, 38(9), 1349. (1992)

HAN, Y. "Modeling and Simulation of Wood Pulp Washers", PhD Dissertation University of Idaho, (1989).

KEMPE, M. J. "Dynamic Modeling of a Vacuum Drum Washing System", Master of Engineering thesis, Dept. of Chemical Engineering, McMaster University, Canada, (1995).

KEREKES, R. J. "Pulp Floc Behavior in Entry Flow to Constrictions" *Tappi*, 66(1), 88. (1983)

KEREKES, R. J.; SCHELL, C. "Effects of Fiber Length and Coarseness on Pulp Flocculation" *Tappi*,78(2), 133. (1995)

LAPPAN, R. E.; HRYMAK, A. N.; PELTON, R. H. "Polymer Enhanced Brownstock Washing: Mill Trial" *Tappi*, 79 (11), 170. (1996)

MEYER, H. "A Filtration Theory for Compressible Fibrous Beds Formed from Dilute Suspensions" *Tappi*, 45, 4. (1962)

PELTON, R. H. "Polymer-Colloid Interactions in Pulp and Paper Manufacture, Colloid Polymer Interactions from Fundamentals to Practice" Edited by Raymond S. Farinato and Paul L. Dubin John Wiley & Sons, Inc. (1999).

OVILLER, O., *Papir-J.*, 26(23), 312. (1938)

RUTH, B.F.; MONTILLON, G. H.; MONTANNA, R. F. "Studies in Filtration I. Critical Analysis of Filtration Theory". *Ind. Eng. Chem.*, 25(76),153. (1933)

SMILE, D. E. "A theory of Constant Pressure Filtration". *Chem. Eng. Sci.*, 25,985. (1970)

STAMATAKIS, K. "Analysis of Cake Formation and Growth in Liquid-Solid Separation PhD Dissertation Syracuse University (1990).

STAMATAKIS, K.; TIEN, C. "Cake Formation and Growth in Cake Filtration". *Chem Eng. Sci.*, 46(8), 1917. (1991)

TILLER, F. M. "Compressible Cake Filtration" pp. 315-397 *The Scientific Basis of Filtration* Edited by Ives, K. J. Noordhoff International Publishing Co. (1975).

TILLER, F. M , Cleveland, T.; Lu, R. "Pumping Slurries Forming Highly Compactible Cakes" *Ind. Eng. Chem. Res.*, 38, 590, (1999)

WAKEMAN, R. J. "A Numerical Integration of the Differential Equations Describing the Formation of and Flow in Compressible Filter Cakes" *Trans I ChemE.*, 56. (1978)

WANG, J.; PELTON, R. H.; HRYMAK, A.; KWON, Y. "New Insights into Dispersed Air Effects in Brownstock Washing". *Tappi*, 84(1), 1. (2001)

WANG, J; HRYMAK, A. N.; PELTON R. H. "Specific Surface and Effective Volume of Water Swollen Pulp Fibers by a Permeability Method."*J. of Pulp Paper Sci.* Vol.28, No. 1 pp 13-16, January, (2002).

WANG, X. "Dynamic Simulation of Brown Stock Washers and Bleach Plants" MS thesis, The University of British Columbia, Vancouver, BC, Canada (1993).

CHAPTER 5

Theoretical and Numerical Solutions for Compressible Fibrous Mat Formation from Dilute Suspensions

SUMMARY:

A new numerical solution for compressible fibrous mat formation from dilute suspension based on traditional filtration theory and recently developed pulp fiber mat permeability model was done. This newly developed numerical model allows the equations to be solved rapidly and with high accuracy. The simulation results agree with industrial mat thickness data and previous experimental measurements and it can be extensively used in pulp and paper industry, such as sheet formation and wet-pressing process for its simplicity and for its accuracy. This is the first direct and complete, filtration theory based, potential industrial applicable, numerical solution for pulp mat formation from dilute suspension.

5.1 INTRODUCTION:

In kraft pulping , wood chips are converted into an aqueous fiber suspension suitable for papermaking. The formation of wood fiber mats from fiber suspension and the flow of water through fiber mats are extensively used in this industry. Examples include rotary vacuum pulp washing sheet formation and wet-pressing. Although this

topic has been studied for many years, there is still no theoretical simulation model for pulp washing, which can be used in industry for process design and optimization. The difficulties are both in model itself and in numerical solution.

Unlike rigid porous media, wood fiber mats are compressible (permeability decreases under compression) and water swollen. Based on traditional filtration theory, a model for fibrous beds formed from dilute suspensions was proposed by Meyer (1962). Although the detailed numerical solution was not provided and a problematic relationship of porosity (negative porosity at higher vacuum level) and fiber concentration was employed, Meyer's work was the first attempt in this area. Jonsson and Jonsson (1992) proposed a dynamic model for wet-pressing, this model can only be used in incompressible isotropic layers. Zhu et al. (1995) proposed a micromechanistic model based on the advances in textile science and engineering. Flow in a model multi-permeability porous media was studied by Lappan et al (1997).

Based on traditional filtration theory and recently developments of pulp fiber mat permeability model a modified Tiller's filtration was developed (Wang et al, 2002). Fiber characteristics were used in the model simulation and the effects of the fiber characteristics on the mat formation process were examined. The discrete numerical equations(Finlayson, 1980) of the underlying PDE model is relatively simple in comparison with Jonsson and Jonsson's (1992) local linearization method with Taylor series expansion and Stamatakis' (1991) numerical approach.

5.2 MODEL DEVELOPMENT:

In traditional filtration theory (Tiller 1975, Stamatakis, 1990), we get the following equations by applying the mass conservation principles from any arbitrary point within a pulp mat.

Conservation of Liquid:

$$\frac{\partial \varepsilon}{\partial t} = \frac{\partial q}{\partial x} \tag{5-1}$$

where, ε is porosity of the mat, t is time, x is distance opposite of flow direction started on filtration screen, q is local water flux (m^3/m^2).

Conservation of Solid:

$$\frac{\partial \varepsilon}{\partial t} = -\frac{\partial q_s}{\partial x} \tag{5-2}$$

where q_s is downward flux of pulp fiber (m^3/m^2)

Darcy's Law, as modified by Shirato et al. (1969), may be expressed in the form

$$\frac{dP_s}{dx} = -\frac{\mu}{K} q_{ls} \tag{5-3}$$

where q_{ls}: the apparent relative liquid to fiber velocity expressed as volume of liquid per unit time and unit cross-section area. dp_s/dx is the pressure gradient on fiber mat. μ is the viscosity and K is the permeability.

The apparent liquid velocity, q, the apparent solid velocity, q_s and the apparent relative liquid velocity to solids, q_{ls} are related according to the expression.

$$q_{ls} = q - \frac{\varepsilon}{1-\varepsilon} q_s \tag{5-4}$$

From equation (5-1) and (5-2) we get

$$\frac{\partial q}{\partial x} + \frac{\partial q_s}{\partial x} = 0 \tag{5-5}$$

$$q + q_s = const \tag{5-6}$$

where q_1: outlet flux

$$q + q_s = q_1 \tag{5-7}$$

Substitute (5-7), (5-4) into (5-3) we get

$$\frac{dP_s}{dx} = -\frac{\mu}{K}[q - \frac{\varepsilon}{1-\varepsilon}(q_1 - q)] \tag{5-8}$$

Rearrange equation (5-8) we get

$$q = \varepsilon q_1 - \frac{1-\varepsilon}{\mu} K \frac{dP_s}{dx} \tag{5-9}$$

Substitute equation (5-9) to (5-1)

$$\frac{\partial \varepsilon}{\partial t} = \frac{\partial}{\partial x}(\varepsilon q_1) - \frac{\partial}{\partial x}[\frac{(1-\varepsilon)k}{\mu}\frac{\partial P_s}{\partial x}] \tag{5-10}$$

Equation (5-10) is commonly accepted in filtration theory, this result has been reported by many other researchers (see, Stamatakis, K. P., 1990)

Given our new porosity consistency model, equation (3-6) or equation (4-3), we have

$$\varepsilon = (1 - \theta_1)^{\gamma c}$$

where $\theta_1 = 4.342 \times 10^{-3}$ for our Northern Canadian unbeaten bleached kraft pulp fiber and γ equals 1.0 (see equation 3-6 or equation 4-3)

From Han's (1969) fiber compressibility model we have

$$c = 1000m(10P_s)^n \tag{5-11}$$

where C is the fiber concentration in kg/m^3 and P_s is mechanical pressure in Pa. The regression of our Northern Canadian unbeaten bleached kraft fiber experimental data of c - p_s (Robertson and Mason,1949) gave m: 0.00271 n:0.3515

From Darcy's law, we can get the outlet flux of water

$$q_1 = [\frac{k}{\mu}(\frac{\partial P_s}{\partial x})]_{x=0} \tag{5-12}$$

Substituting equations (3-6), (5-12) into equation (5-10) we obtain

$$\frac{\partial c}{\partial t} = [a(c)\frac{\partial c}{\partial x}]_{x=0}\frac{\partial c}{\partial x} - b(c)\frac{\partial}{\partial x}[d(c)\frac{\partial c}{\partial x}] \tag{5-13}$$

where

$$a(c) = \frac{k}{10\mu n}\left(\frac{1}{1000m}\right)^{1/n} c^{1/n-1} \tag{5-14}$$

$$b(c) = \frac{1}{(1-\theta_1)^c \ln(1-\theta_1)} \tag{5-15}$$

$$d(c) = \frac{[1-(1-\theta_1)^c]k}{\mu}\frac{1}{10n}\left(\frac{1}{1000m}\right)^{1/n} c^{1/n-1} \tag{5-16}$$

In order to simplify the numerical solution process, we do a similarity transformation (Finlayson, 1980) by defining

$$\eta = \frac{x}{t^{\frac{1}{2}}} \tag{5-17}$$

Substituting equation (5-17) into (5-13) we can turn the partial differential equation to ordinary differential equation,

$$-\frac{\eta}{2}\frac{dc}{d\eta} = [a(c)\frac{dc}{d\eta}]_{\eta=0}\frac{dc}{d\eta} - b(c)[e(c)(\frac{dc}{d\eta})^2 + d(c)\frac{d^2c}{d\eta^2}] \tag{5-18}$$

where

$$e(c) = \frac{d(d(c))}{dc} = \frac{1}{10\mu nkS_0^2}\left(\frac{1}{1000m}\right)^{1/n}[(1/n-1)c^{1/n-2}\frac{(1-\theta_1)^{3c}}{1-(1-\theta_1)^c}$$
$$+ c^{1/n-1}[\frac{3(1-\theta_1)^{3c}\ln(1-\theta_1)}{1-(1-\theta_1)^c} + \frac{(1-\theta_1)^{4c}\ln(1-\theta_1)}{[1-(1-\theta_1)^c]^2}] \tag{5-19}$$

The discretized numerical solution of ordinary differential equation (5-18):

$$\frac{dc}{d\eta} = \frac{c_{n+1} - c_n}{\Delta\eta} \tag{5-20}$$

in which

$$\frac{d^2c}{d\eta^2} = \frac{c_{n+1} - 2c_n + c_{n-1}}{(\Delta\eta)^2} = \frac{c_{n+1} - 2[\Delta\eta \frac{dc}{d\eta} + c_{n-1}] + c_{n-1}}{(\Delta\eta)^2} \tag{5-21}$$

$$c_{n+1} = 2[\Delta\eta \frac{dc}{d\eta} + c_{n-1}] - c_{n-1} + (\Delta\eta)^2 [\frac{\frac{1}{2}\eta \frac{dc}{d\eta} + [a(c)\frac{dc}{d\eta}]_{\eta=0} \frac{dc}{d\eta}}{b(c)d(c)} - \frac{e(c)}{d(c)}(\frac{dc}{d\eta})^2]$$

(5-22)

with the following boundary condition:

$$\eta = 0; \quad c = 1000m(10P_s)^n$$

The resistance of the filtration screen was neglected because the resistance of metal screen is considered to be much smaller than that from cake. Jonsson and Jonsson (1992) also neglected the resistance of metal screen.

$$\eta = \infty; \quad c = 8kg/m^3$$

With both boundary conditions, equation 5-22 can be solved.

5.3 RESULTS AND ANALYSIS

A series of simulations at varied operating conditions have been conducted. The sample base case parameters are listed in Table 5-1. The 19 cases, that were correspond to changes in one parameter while keeping the other parameters to the same as that in the base case. The simulation results were plotted on Figure. (5-1) to (5-8).

Table 5-1. Parameters and cases in the simulation

Variables	Sample base case	Other cases
Time	5.0 seconds	1,2,5,10,20,30,60 seconds
Vacuum	10.0 kPa	10.0, 20.0, 30.0, 66.7 kPa
S_0*	2.7145×10^5 m^2/m^3	1,2,5,10 times of S_0
θ_1*	0.004342	0.5, 1.0, 1.5 times of θ_1
Fiber Concentration in the Slurry	8.0 kg/m3	8.0, 10.0, 12.0 kg/m3
Viscosity	0.009 Pa.s	1, 2, 5 times of Standard

*θ_1 is the volume fraction of swollen fiber at a fiber concentration of 1.0kg/m3

* S_0 is surface area per unit volume of solids (m^2/m^3)

Lappan et al. (1997) reported that a 40 mm thick fiber pad is formed by filtration on the screen of a large slowly (about 4 rpm) rotating vacuum drum. Usually about 40% of the drum surface is under water in the vat, so the mat formation process in the industry occurs in about 6 seconds. Our standard case, shown in Figure 5-1, simulates the case of 5 seconds of mat formation time. The calculation predicts a mat thickness of about 70 mm,

which is higher than that of the typical mat formed on a rotary drum washer. The calculated fiber pad thickness is reasonable, by considering the presence of lignin and air bubbles in the industry process, which lows the mat permeability and slows the pulp load (see the following analysis). Following are detailed list of the analysis of effects on different variables.

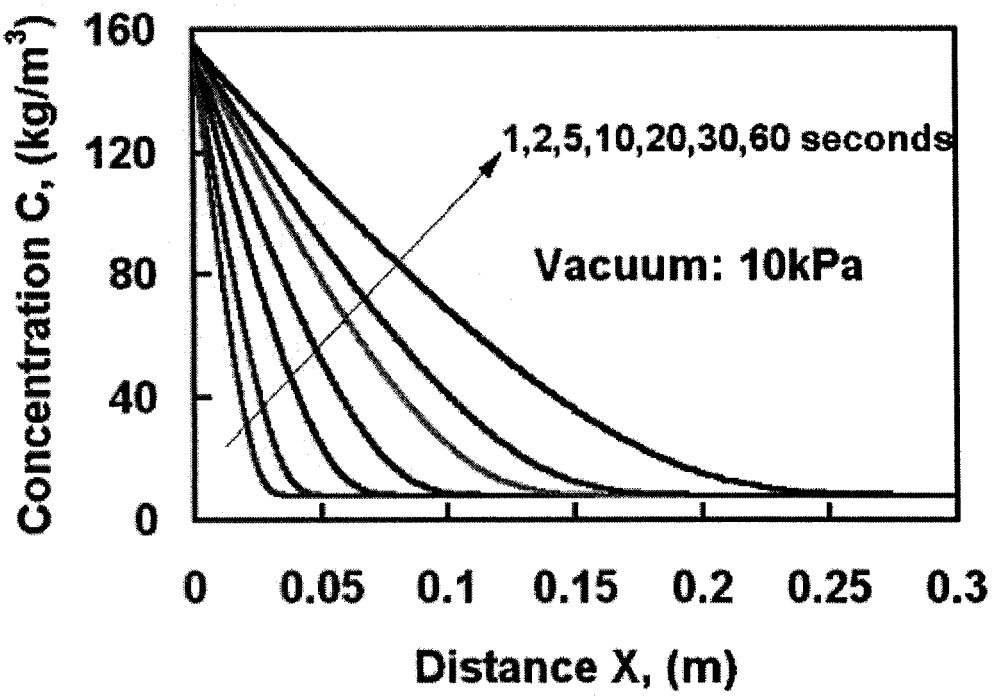

Figure 5-1. Dynamic profiles of mat concentration distribution

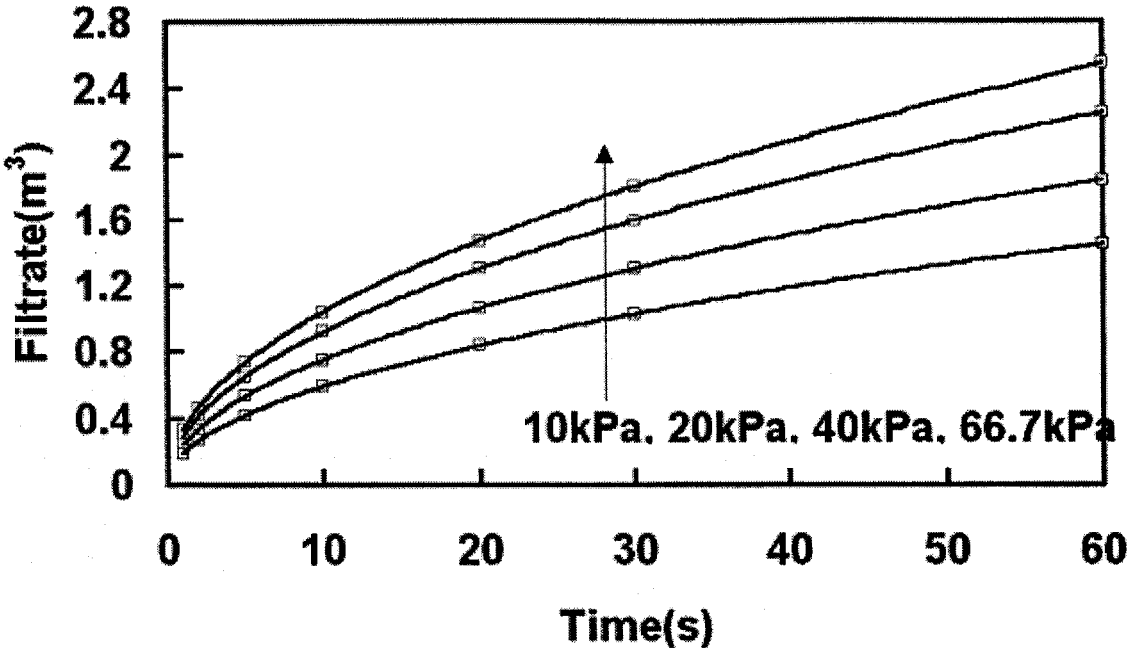

Figure 5-2. Filtrate at various vacuum levels as a function of time

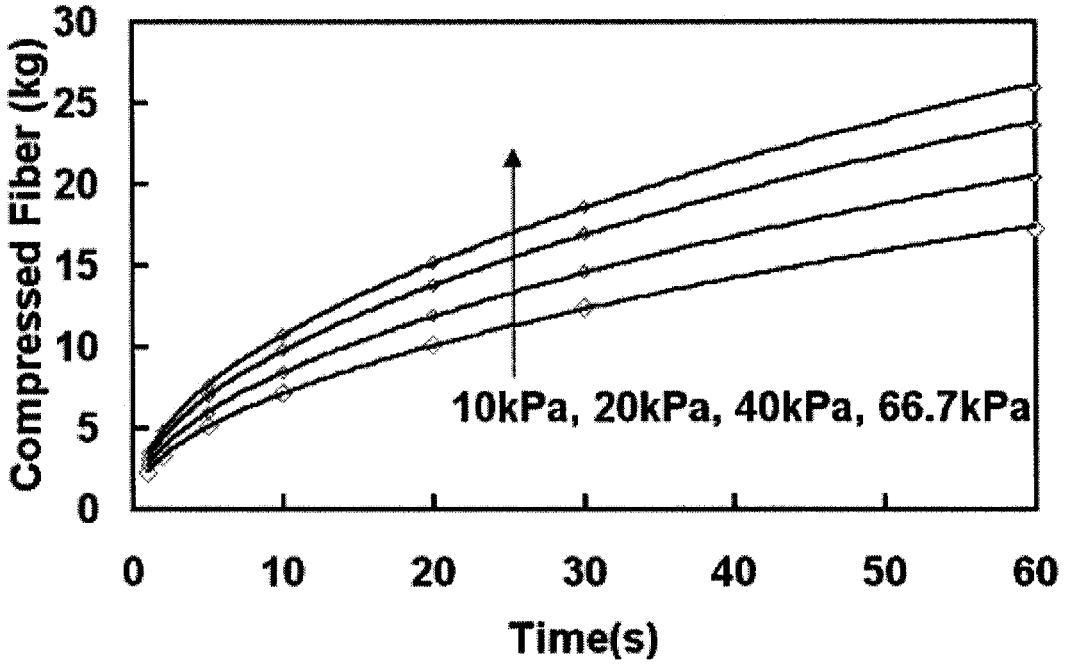

Figure 5-3. Total mass of fibers on per square meter of surface of screen as a function of time

A) Time

In the industrial design and operation of rotary drum washers, operating time affects the size of the equipment to maintain a given production and is controlled by the rotary speed. In Figure 5-1, the areas under the curves (integration of fiber concentration profiles) correspond to total mass of fiber above the filtration screen of unit filtration screen area. If we look at the curves at 1 second and 5 seconds, we can find that productivity of unit filtration screen area of 5 seconds is much smaller than that of 5 times of 1 seconds.

B) Vacuum

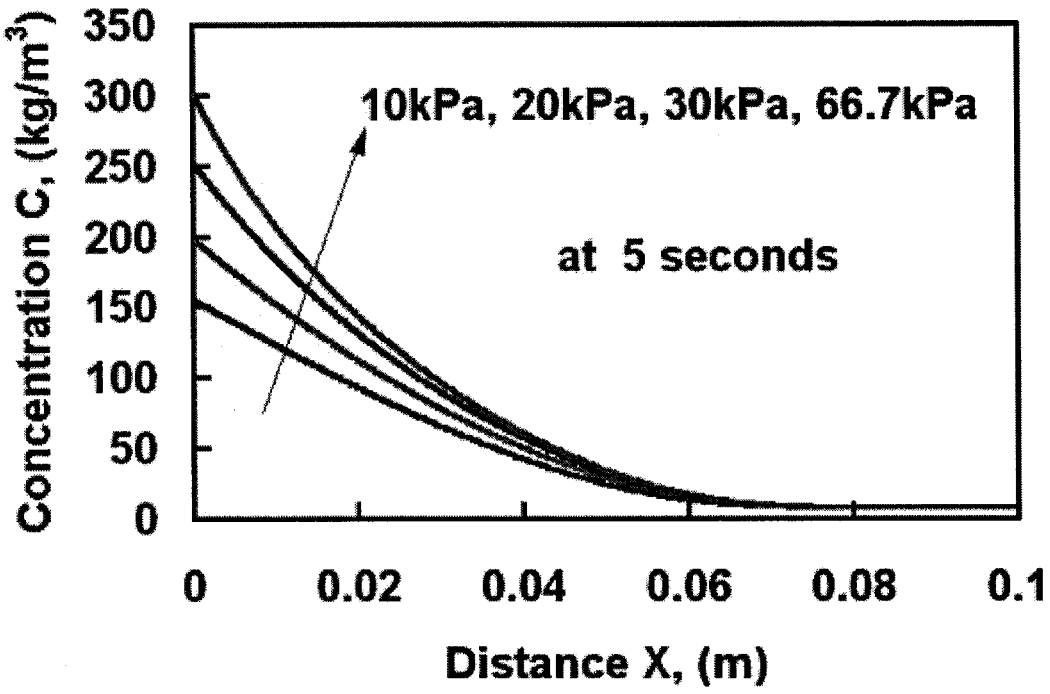

Figure 5-4. The effect of vacuum level on mat formation

In Figure 5-4, it is clear that mat thickness is weakly dependent on vacuum levels. This simulation result agrees with our experimental result. Although increasing vacuum level will increase the pulp loading, it is not a very efficient way to do so. So the vacuum level is always kept to the least required maintain the filtrate flow needed for the production requirement.

C) Fiber Surface Area (S_0)

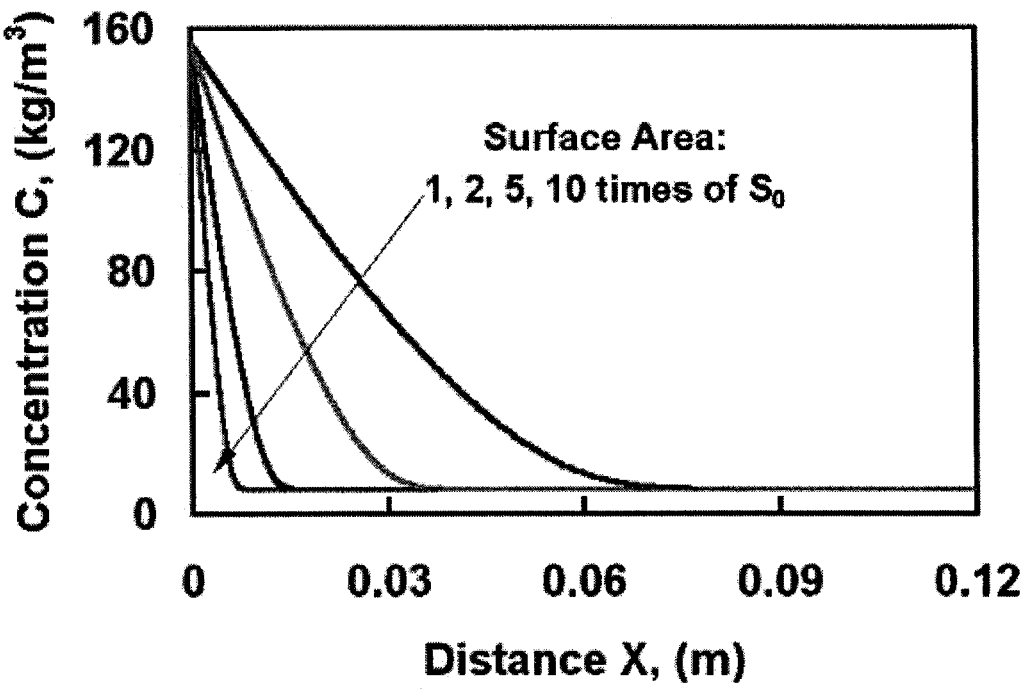

Figure 5-5. The effect of surface area of fiber on mat formation

In Figure 5-5, we can see that fibers with larger surface area reduce the unit productivity of washer. The unit pulp loading on the drum of a washer can be defined as the total mass of fiber on a unit filtration screen or the area under the appropriate curve on concentration profile plots. So fiber surface area (corresponding to "fiber beaten"

operation) dramatically slows the process. If we would like to have a higher unit productivity for our washers, "fiber beaten" may take place after washing process, this is exactly meet present industry practice.

D) Fiber Water absorption Property (θ_1)

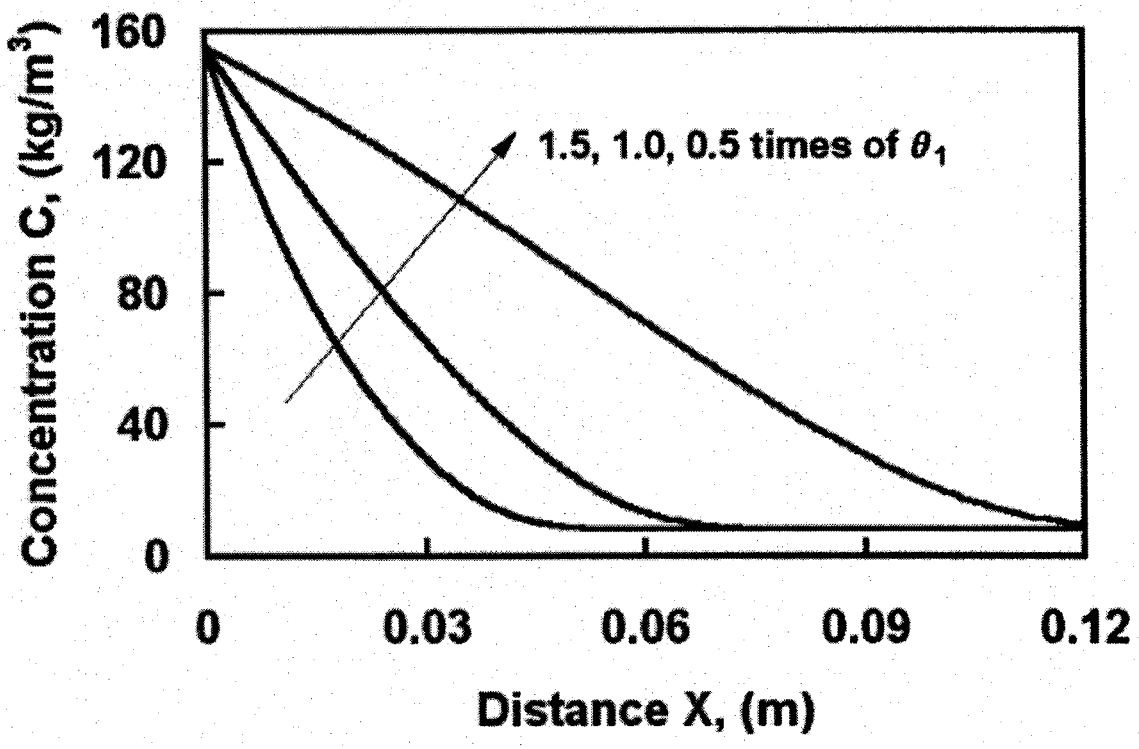

Figure 5-6 The effect of water absorption parameter (θ_1) on mat formation

In Figure 5-6, highly water swollen fiber dramatically reduce the unit productivity of a washer. The relationship between our water swell parameter θ_1 and conventional water swell parameter α and fiber concentration C was shown in equation 3-7.

E) Fiber concentration in pulp slurry

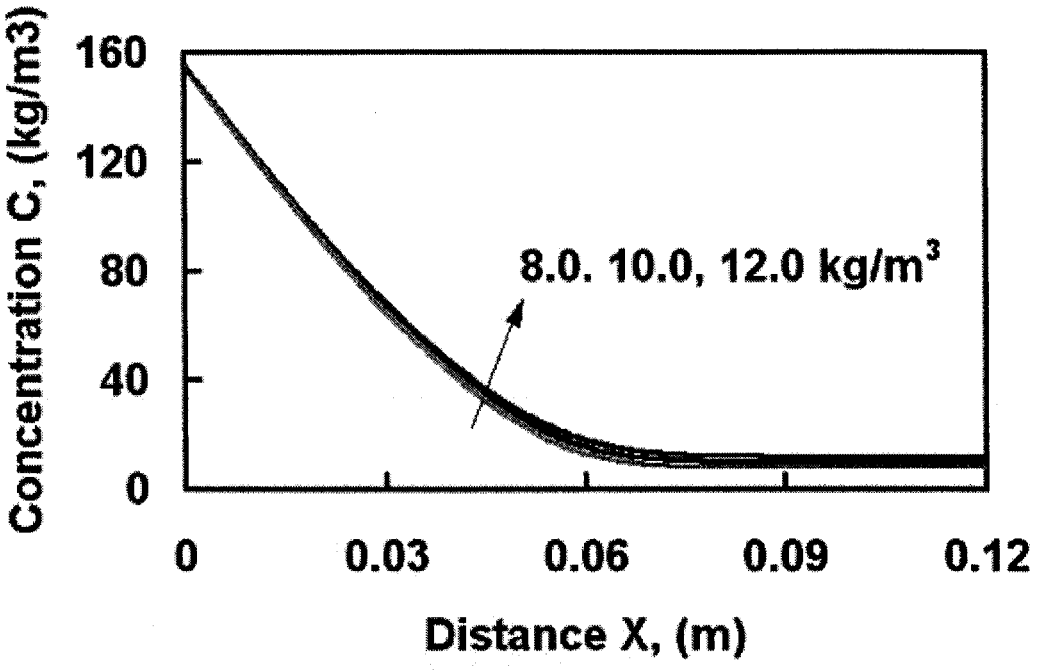

Figure 5-7 The effect of pulp slurry concentration on mat formation

In Figure 5-7, it is clear that small adjustment of fiber concentration in pulp slurry does not have much influence of the unit productivity in terms of pulp throughput.

F) Viscosity of liquid phase

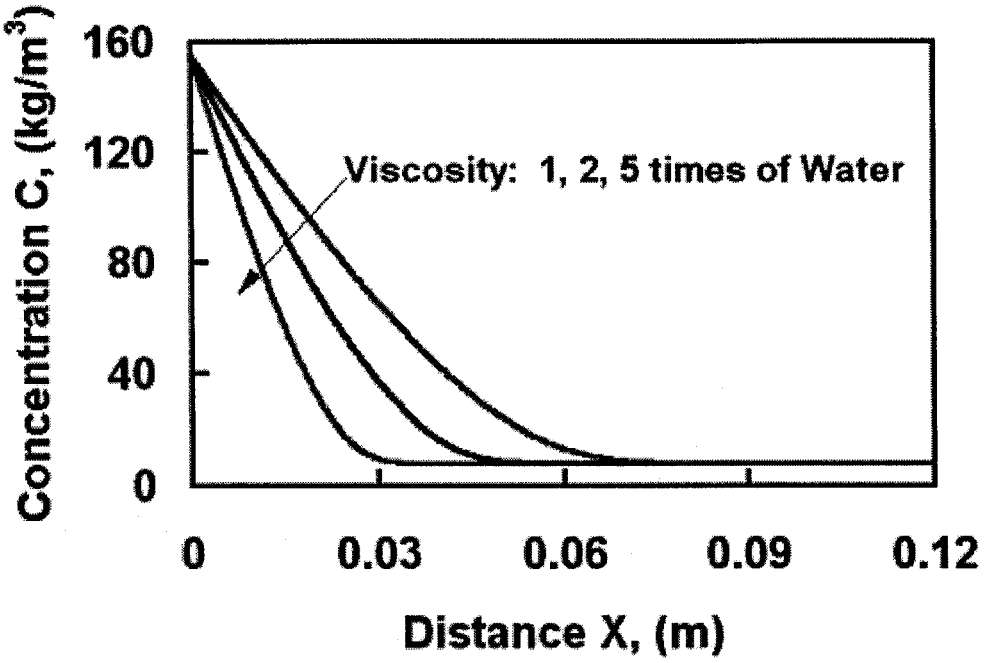

Figure 5-8. The effect of viscosity of liquid phase on mat formation

In Figure 5-8, it is clear that higher fluid phase viscosity reduces the unit pulp throughput. For the case of pure water in liquid phase we can see that the mat thickness is about 70 mm. In the industry, lignin exists in significant quantities in the liquid phase , so the viscosity of liquid phase will be higher than that of pure water, this will result in reducing the unit productivity. Viscosity decreases with increasing temperature , so this suggests that a higher operating temperature will increase the unit productivity of a washer.

5.4 CONCLUSIONS:

A numerical solution using a similarity transform was developed for the flow equations based on traditional filtration theory and a recently developed fiber permeability model. The simulation results of the trend of mat thickness and filtrate data agreed with our experimental measurements. The mat thickness data is also reasonable in comparison with industrial data. Other variables in the model, such as viscosity, fiber surface area, fiber water absorption, pulp suspension concentration, were tested and the results look very reasonable.

REFERENCES:

FINLAYSON, B. A. "Nonlinear Analysis in Chemical Engineering" McGraw-Hill, (1980)

HAN, S. T. "Compressibility and permeability of Fiber Mats" *Pulp Paper Mag. Can.* pp.65-77 May (1969)

JONSSON, K. A. and JONSSON, B. T. L."Fluid Flow in Compressible Porous Media: II Dynamic Behavior"" *AIChE J.* Vol.38, No. 9 pp.1349-1356, September (1992)

LAPPAN, R.; HRYMAK, A. N. and PELTON, R. H. "Dependence of in situ precipitate deposition of flow characteristics in multi-permeability porous media" *Chem. Eng. Sci.*, Vol. 52, No.17, pp. 2963-2975, (1997)

MEYER, H. "A Filtration Theory for Compressible Fibrous Beds Formed from Dilute Suspensions" *Tappi* Vol.45, No.4, April (1962)

SHIRATO M.; SAMBUCHI M. ; KATO H. and ARAGAKI, T. "Internal Flow Mechanism in Filter Cakes" *AIChE J.*, 15, 405-409, (1969)

STAMATAKIS, K. P. "Analysis of cake formation and growth in liquid-solid separations" PhD dissertation, Syracuse University (1990).

TILLER, F. M. "The Scientific Basis of Filtration" edited by K. J. Ives Noordhoff International Publishing, (1975)

WANG, J; PELTON, R. H., HRYMAK, A. and KWON, Y., "New insights into dispersed air effects in brownstock washing" *Tappi*, , Vol:84, No. 1 pp 1-8 January (2001)

WANG, J, HRYMAK, A, AND PELTON, R. "Specific Surface and Effective Volume of Water Swollen Pulp Fibers by a Permeability Method" accepted for publication for, *J. Pulp Paper Sci.* January (2002)

ZHU, S. PELTON, R. H. and COLLVER, K. "Mechanistic Modelling of Fluid Permeation through Compressible Fiber Beds" *Chem. Eng. Sci.,* Vol. 50, No.22, pp3557-3572 (1995)

CHAPTER 6

CONTRIBUTIONS OF THIS WORK

BUBBLE BEHAVIOR OBSERVATIONS:

The first direct observation of dispersed air effects on pulp washing indicated the mechanism by which defoamer increases the water drainage. Channels created by rising large bubbles leave the mat through the screen, while small bubbles tend to be trapped in fiber mat pores. These observations provided understanding of the mechanics of the pulp washing process and may be helpful for further developing models for better industrial design and optimization.

PULP FIBER PERMEABILITY MODELING:

A new pulp fiber permeability model was developed which predicted behavior over a wide fiber concentration range (108 - 415 kg/m^3). This model was essential for studies of mat formation from dilute pulp suspensions. The model provided estimates of the swollen fiber specific surface area and the effective specific volume which are functions of pad consistency.

EXPERIMENTS OF PULP MAT FORMATION:

A systematic experimental investigation of the formation of compressible fibrous mats formed from dilute pulp suspensions has been completed over a range of vacuum levels.

Fiber concentration profiles along the mat formation direction were inferred from the images using a grayscale analysis calibrated against a set of known concentrations. The experiments reports in this thesis captured dynamic fiber concentration distribution in the pulp mat, the filtrate flux and the mat thickness, as a function of time and operating vacuum. Such measurements have not been reported previously in the literature.

MODELING OF PULP MAT FORMATION

A major achievement of this work was a new numerical description of the formation of compressible fibrous mat from dilute fiber suspensions. This model is superior to previous attempts and the numerical model can be solved rapidly and with high accuracy. The simulation results agreed with industrial mat thickness data and our experimental measurements. Furthermore, the model may be applicable to sheet formation and wet-pressing processes during papermaking.